Central Alps

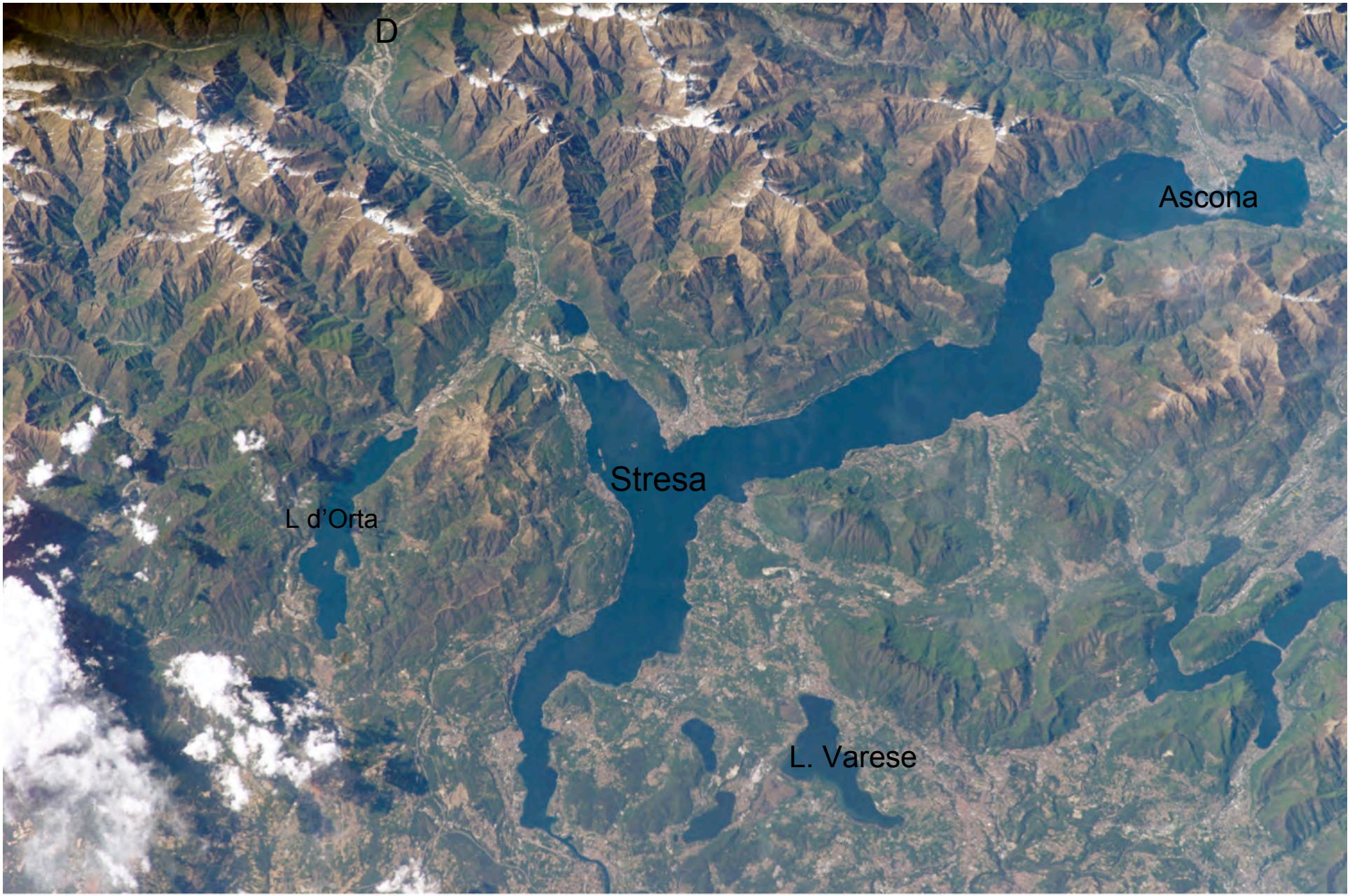

ISS004E10699

Italian Alps: Lago Maggiore

http://eol.jsc.nasa.gov/

Isola Bella, Lago Maggiore view to north

ISS004E11806

Alps: Lake Leman, Rhone Valley, Monte Bianco http://eol.jsc.nasa.gov/

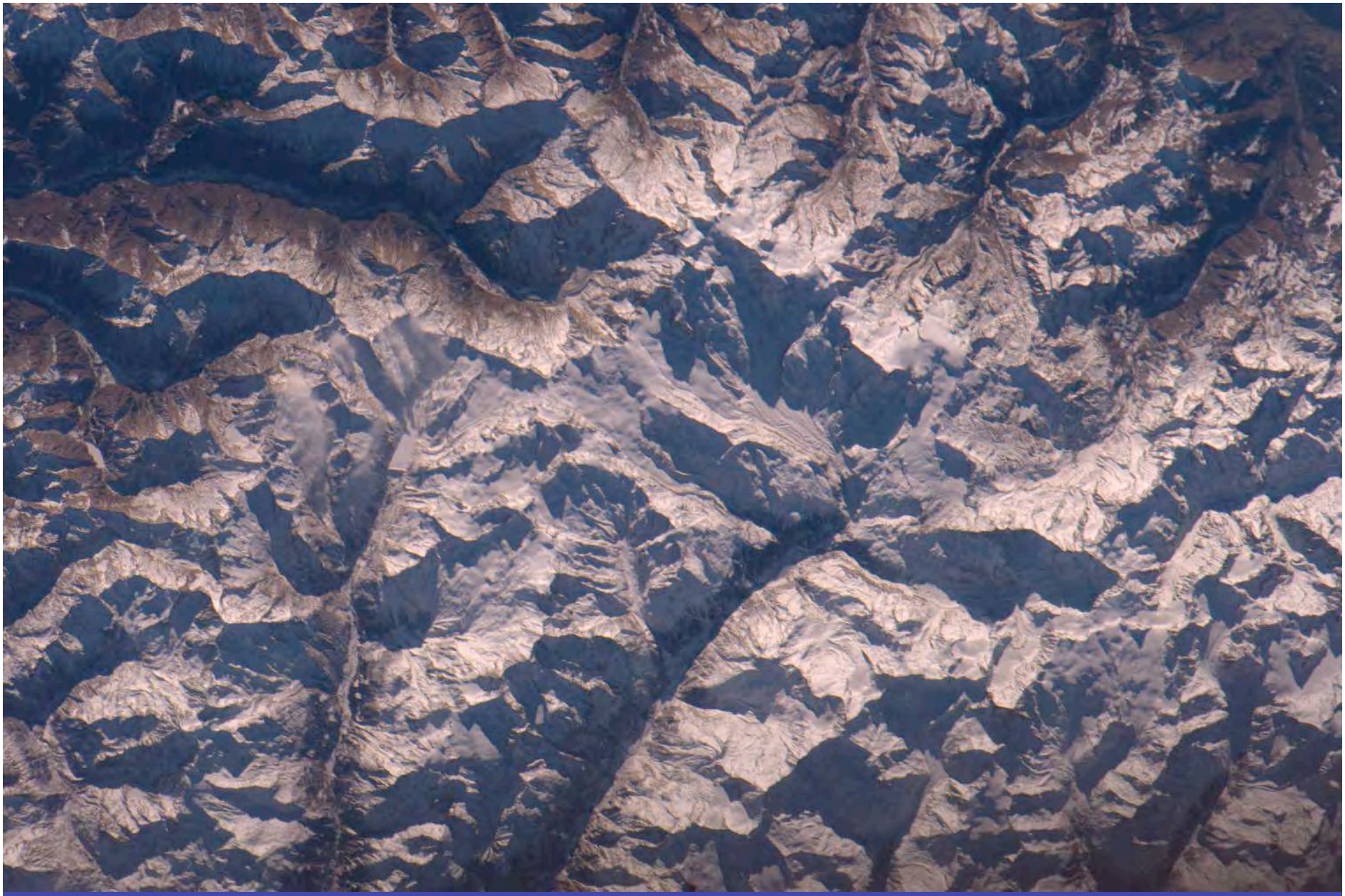

Alps: Zermatt, the Matterhorn

http://eol.jsc.nasa.gov/

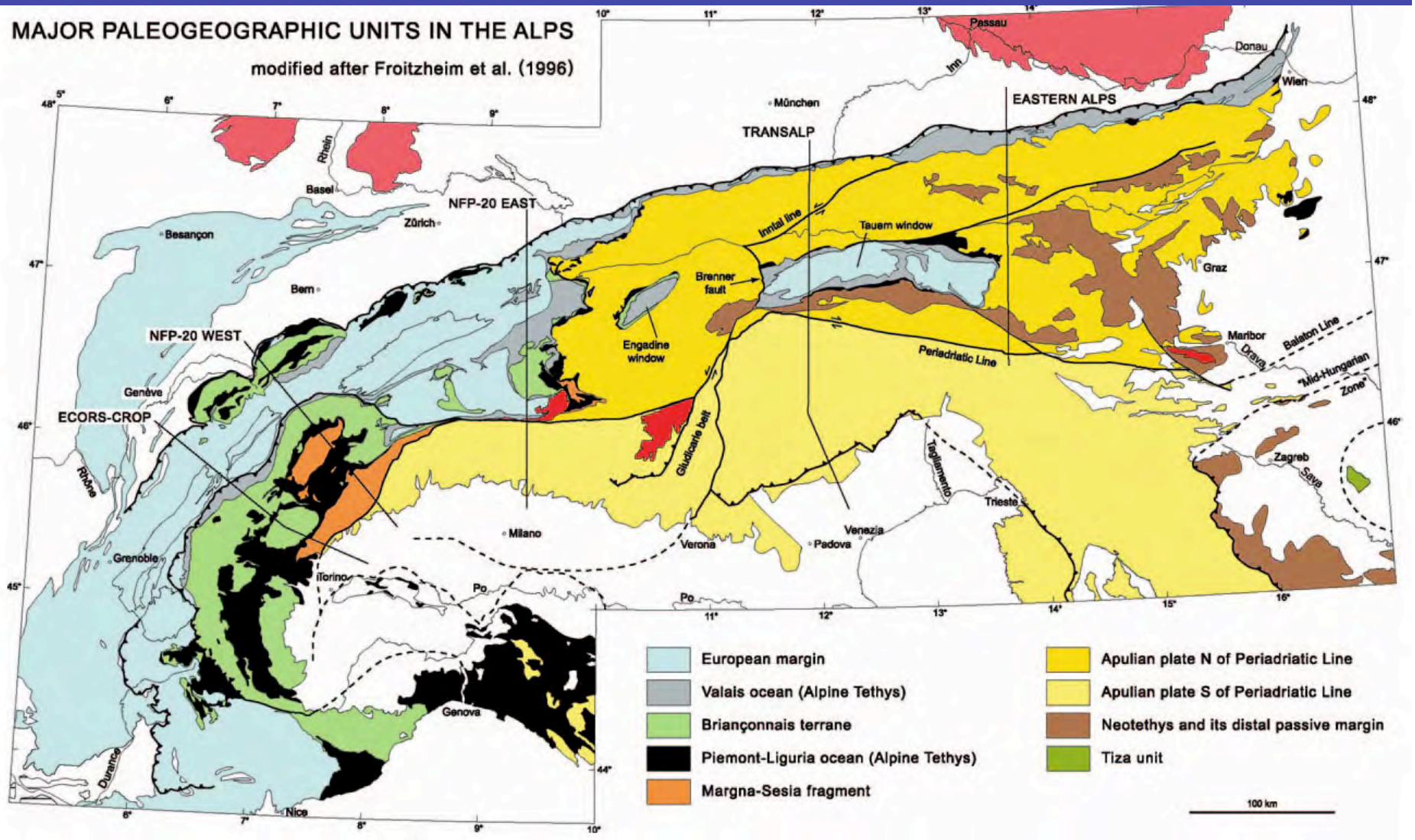

Fig. 1. Map of the major paleogeographic and tectonic units in the Alps.

Schmidt et al 2004

Alpine Crustal Profiles

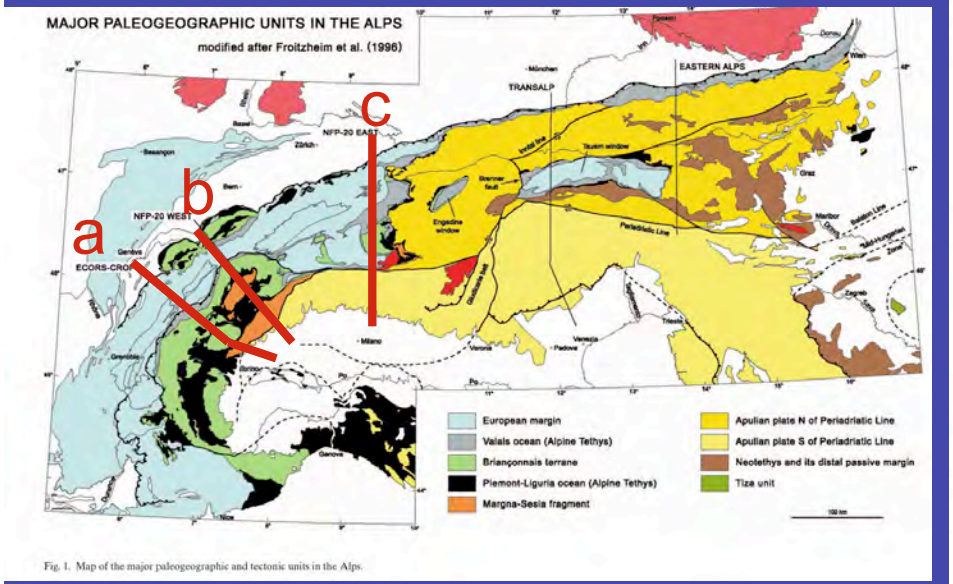

Fig. 1. Map of the major paleogeographic and tectonic units in the Alps.

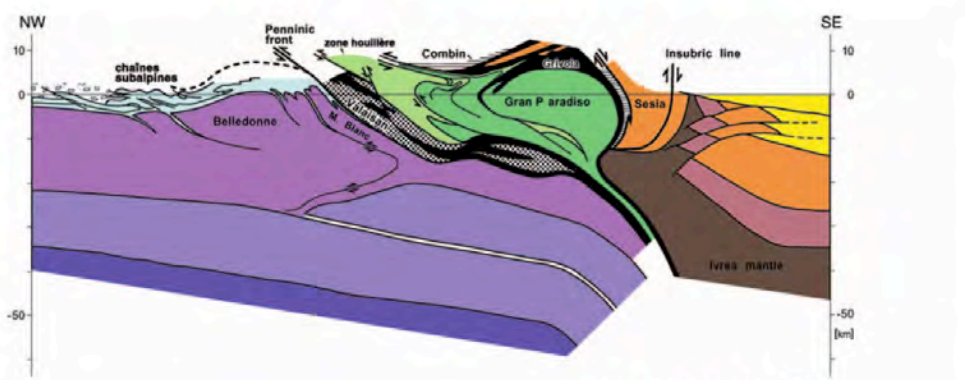

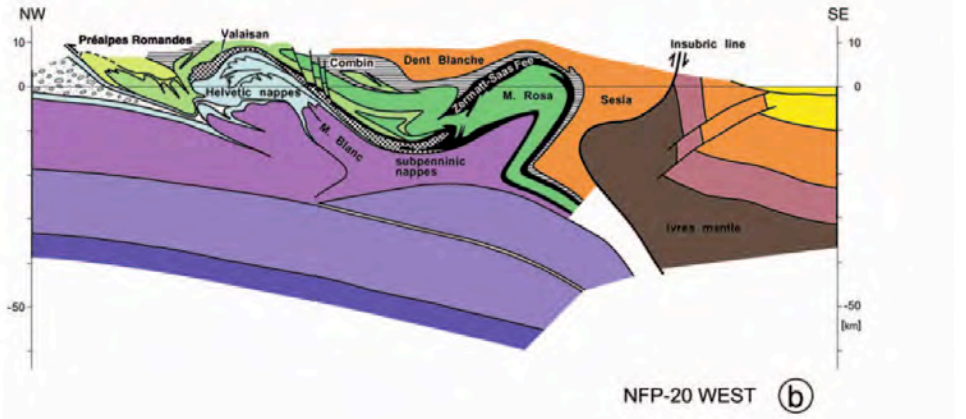

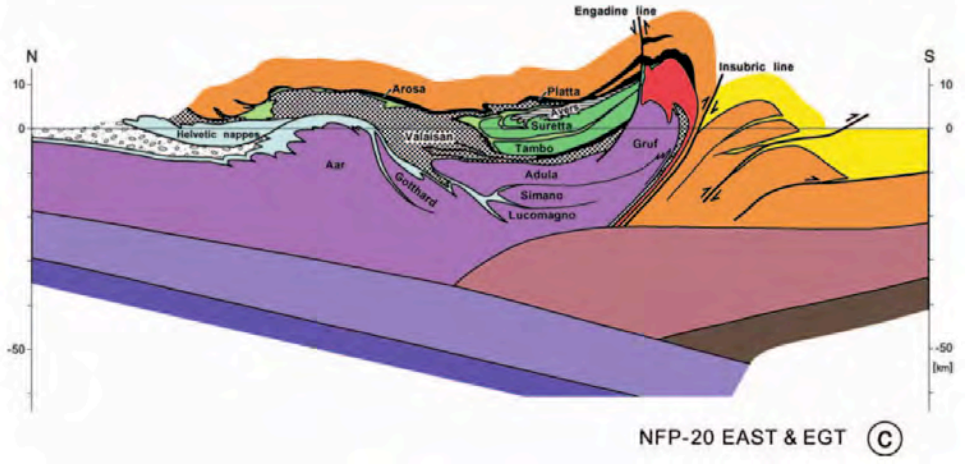

Schmidt et al 2004

Alpine Crustal Profiles

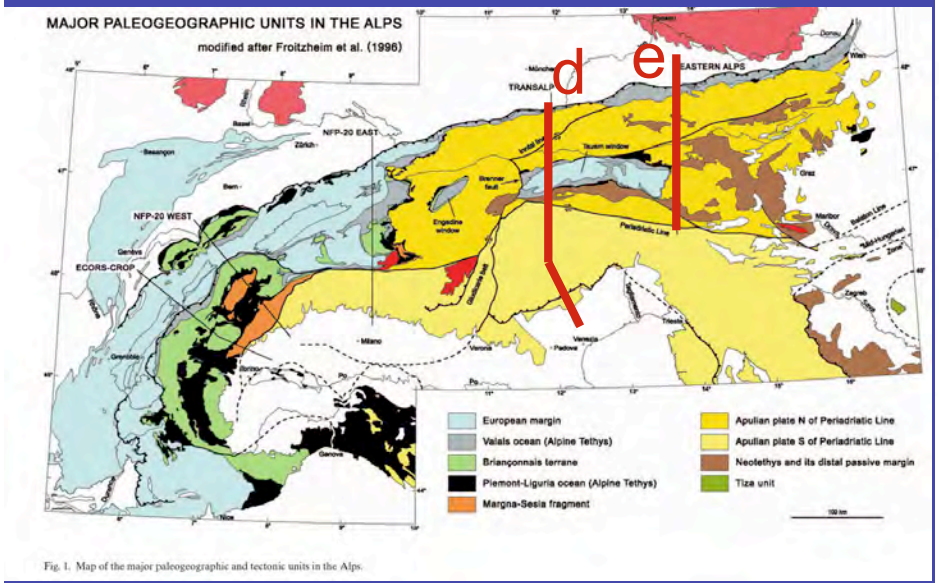

Fig. 1. Map of the major paleogeographic and tectonic units in the Alps.

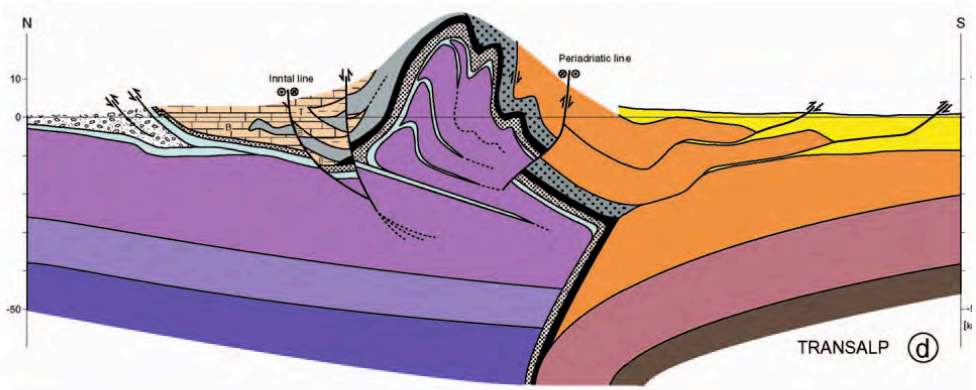

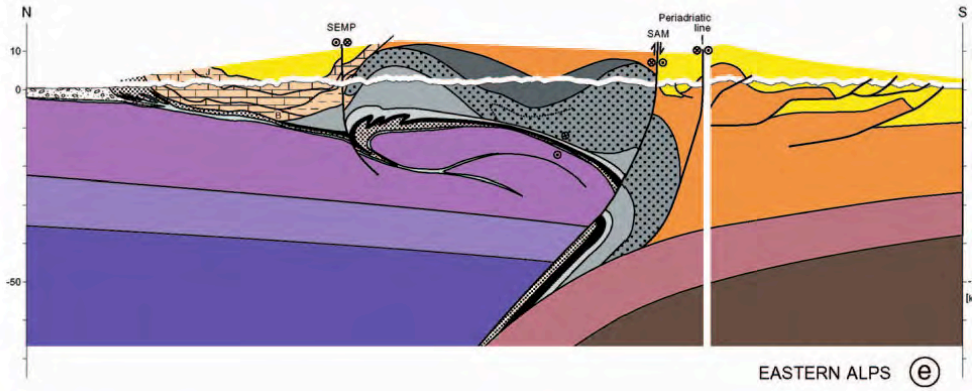

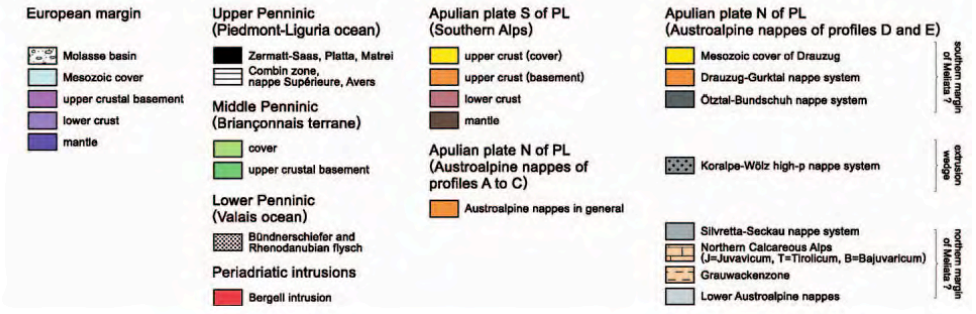

Schmidt et al 2004

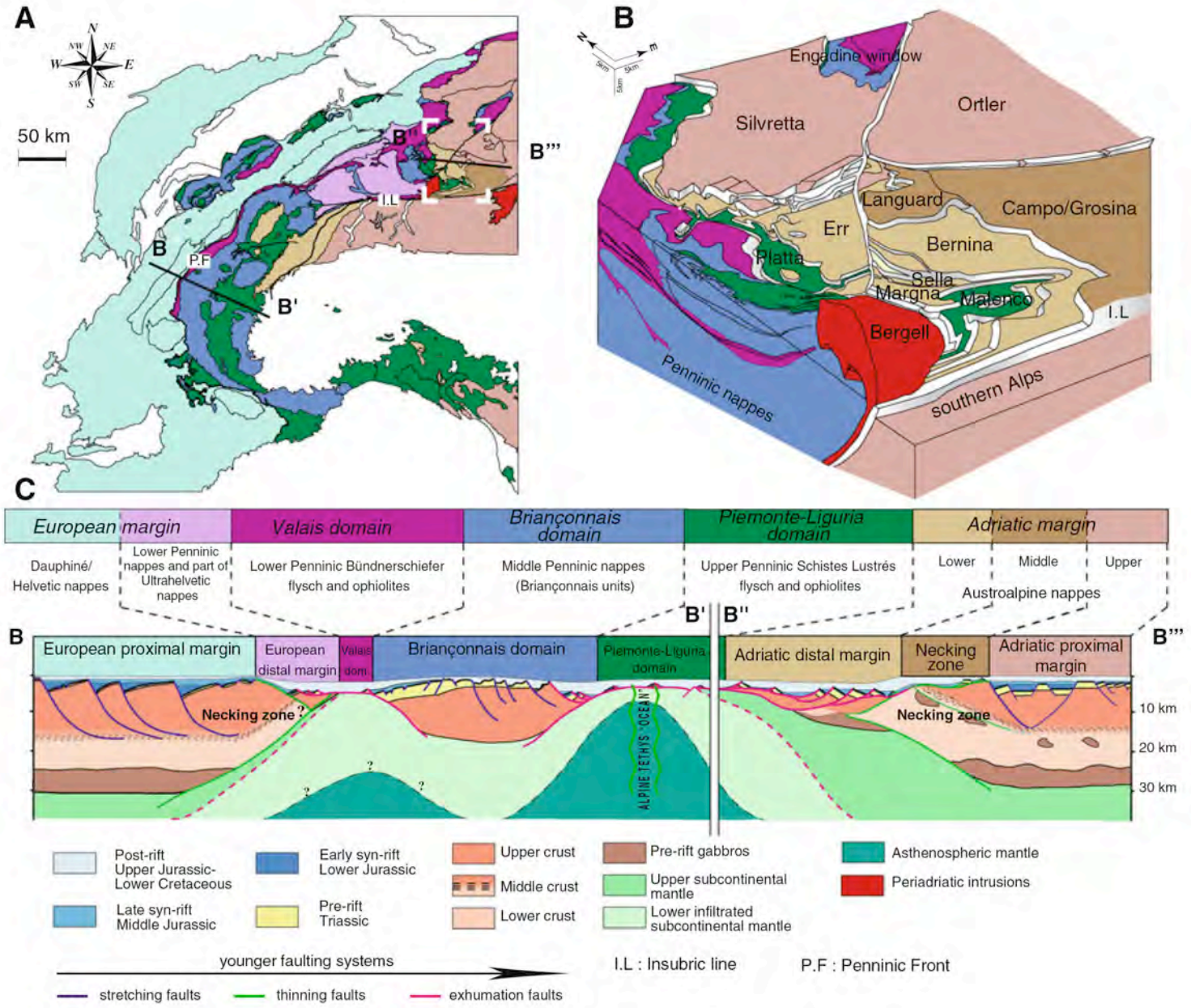

Fig. 2 **a** Tectonic overview map of the Alps showing the distribution of the main paleogeographic domains (modified after Schmid et al. 2004). **b** Schematic block diagram of SE-Switzerland and N-Italy showing the position of the Austroalpine and Penninic nappes and associated units (modified after Froitzheim et al. 1994). **c** Cross-section across the Alpine Tethys margins at the end of rifting and before onset of Alpine convergence in Late Cretaceous time (modified from Mohn et al. 2010). For the location of the cross-section see tectonic map above (**a**)

Mohn et al 2010

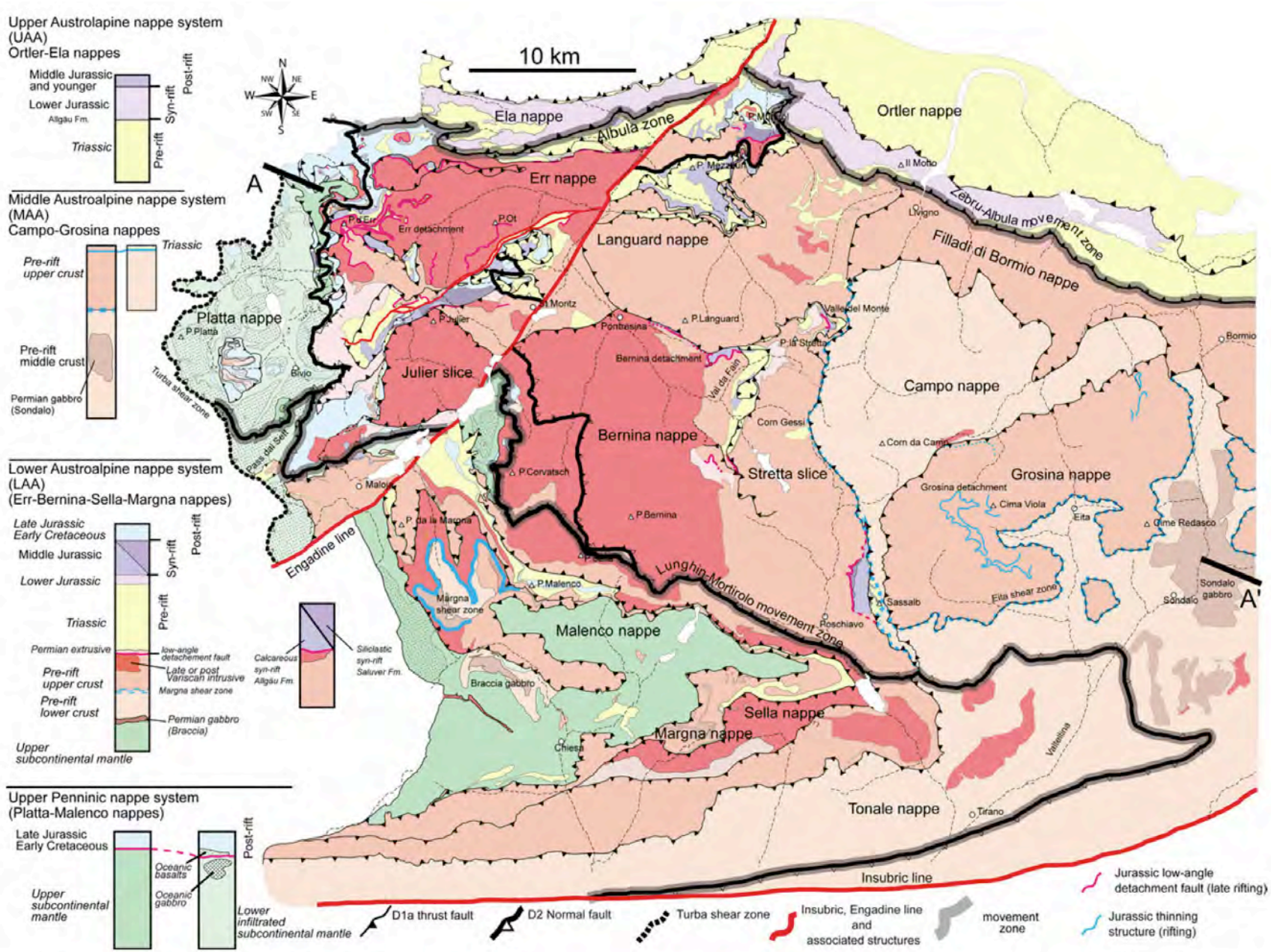

Fig. 3 Geological map of the Austroalpine and Upper Penninic nappes in SE-Switzerland and N-Italy, between Valtelina, Albula, and Julier valleys. Map compiled after Cornelius (1932, 1935, 1950), Staub (1946), Bonsignore et al. 1969a, b, Montrasio et al. 1969, Bearth et al. (1987), Liniger (1992), Spillmann (1993, 2005), Froitzheim et al. (1994), Manatschal (1995), Meier (2003), Trommsdorff et al. (2005) and Peters (2005, 2007) and own observations

Mohn et al 2010

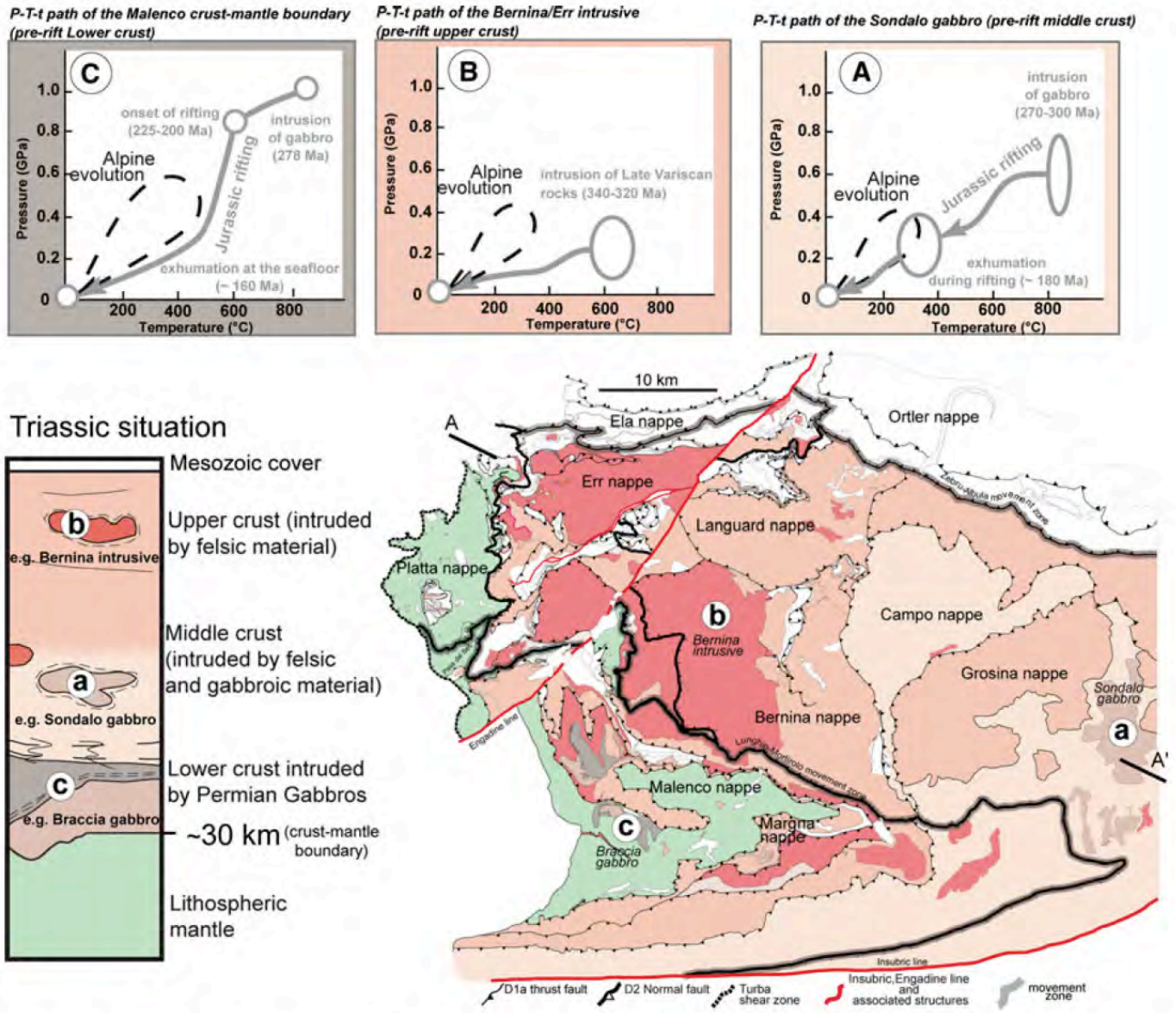

Fig. 4 Alpine tectonic map of the study area showing the distribution of the major nappes discussed in this paper. The section to the right shows a simplified cross-section through the crust in later Permian time, indicating the original position of the rocks found today in the different tectonic units. The P–T-t paths are shown for **a** pre-rift middle crustal gabbros (Sondalo gabbro Tribuzio et al. 1999; Braga et al. 2001, 2003; Meier 2003); **b** pre-rift upper crustal granitoid (Bernina and Err intrusives (Peters 2005, 2007)); **c** pre-rift lower crustal rocks (Malenco crust—mantle boundary (Müntener et al. 2000; Villa et al. 2000)). The data highlight the exhumation during Jurassic rifting of middle and lower crustal rocks. Note that based on the distribution of Alpine metamorphism and thermo-chronological data two nappes edifices can be distinguished that are separated by the Lunghin—Mortirolo movement zone (see text)

Mohn et al 2010

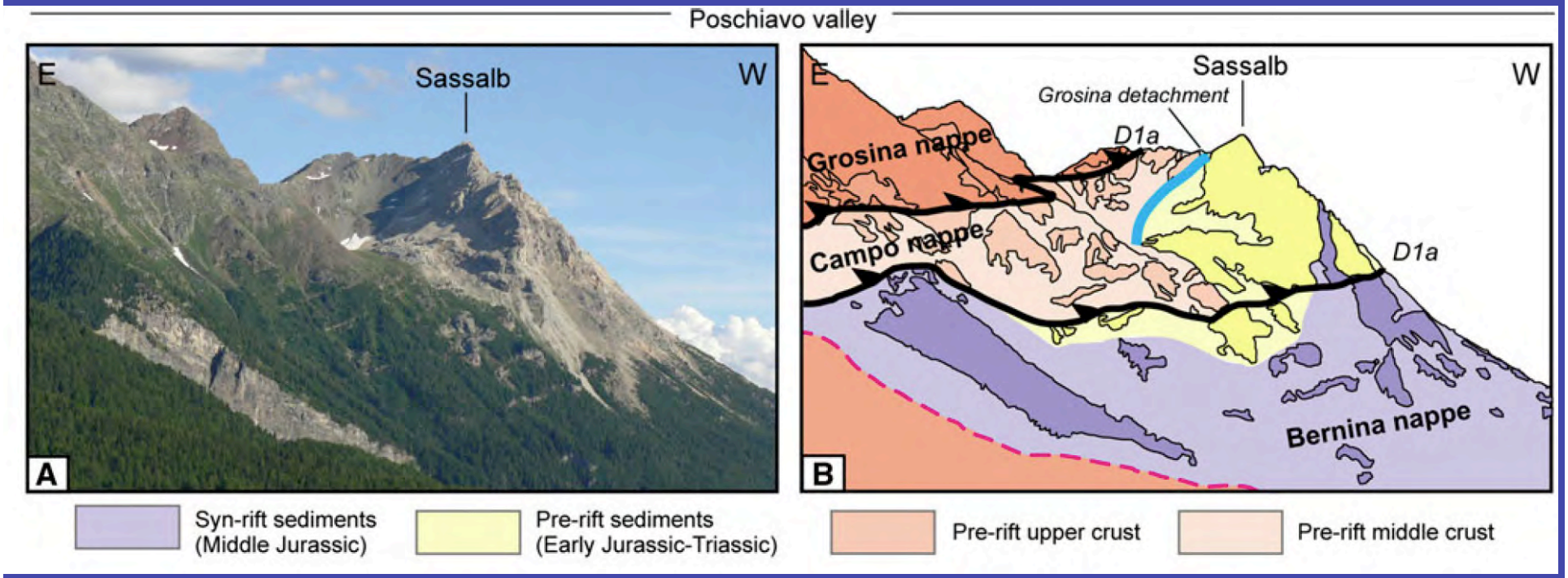

Fig. 9 a, b Photograph and line drawing from the Sassalb area (for localization of the photograph see Fig. 8) showing the contact between Campo-Grosina and Bernina nappes. Crucial observations are that Bernina are juxtaposed against the Campo nappe before Alpine convergence (*blue fault*) and these two units were subsequently trusted by the Grosina nappe during the D1a Alpine phase (see text) (804703/135827, Swiss topographic coordinates). c View of

Mohn
et al 2010

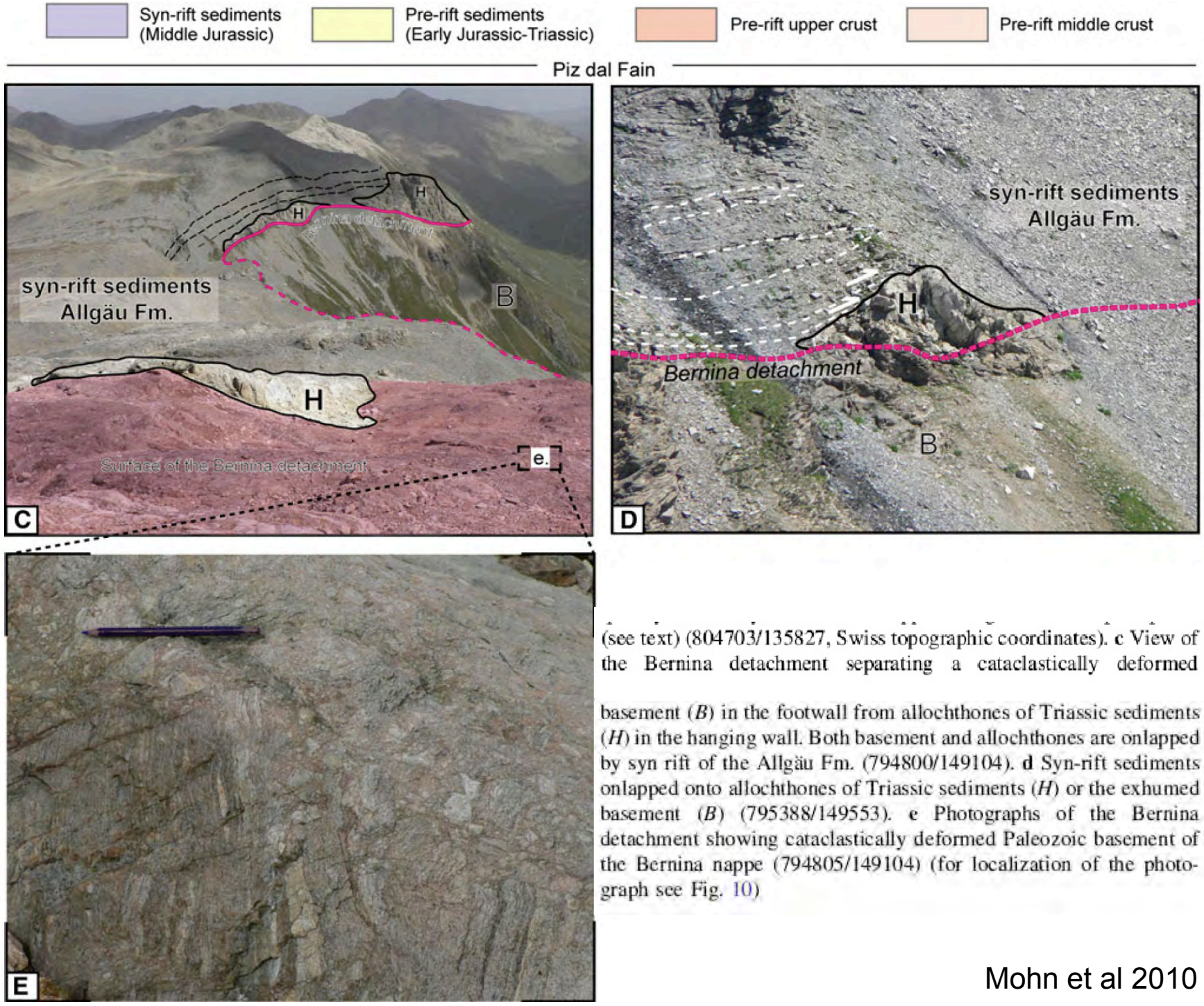

(see text) (804703/135827, Swiss topographic coordinates). **c** View of the Bernina detachment separating a cataclastically deformed basement (*B*) in the footwall from allochthones of Triassic sediments (*H*) in the hanging wall. Both basement and allochthones are onlapped by syn rift of the Allgäu Fm. (794800/149104). **d** Syn-rift sediments onlapped onto allochthones of Triassic sediments (*H*) or the exhumed basement (*B*) (795388/149553). **e** Photographs of the Bernina detachment showing cataclastically deformed Paleozoic basement of the Bernina nappe (794805/149104) (for localization of the photograph see Fig. 10)

Mohn et al 2010

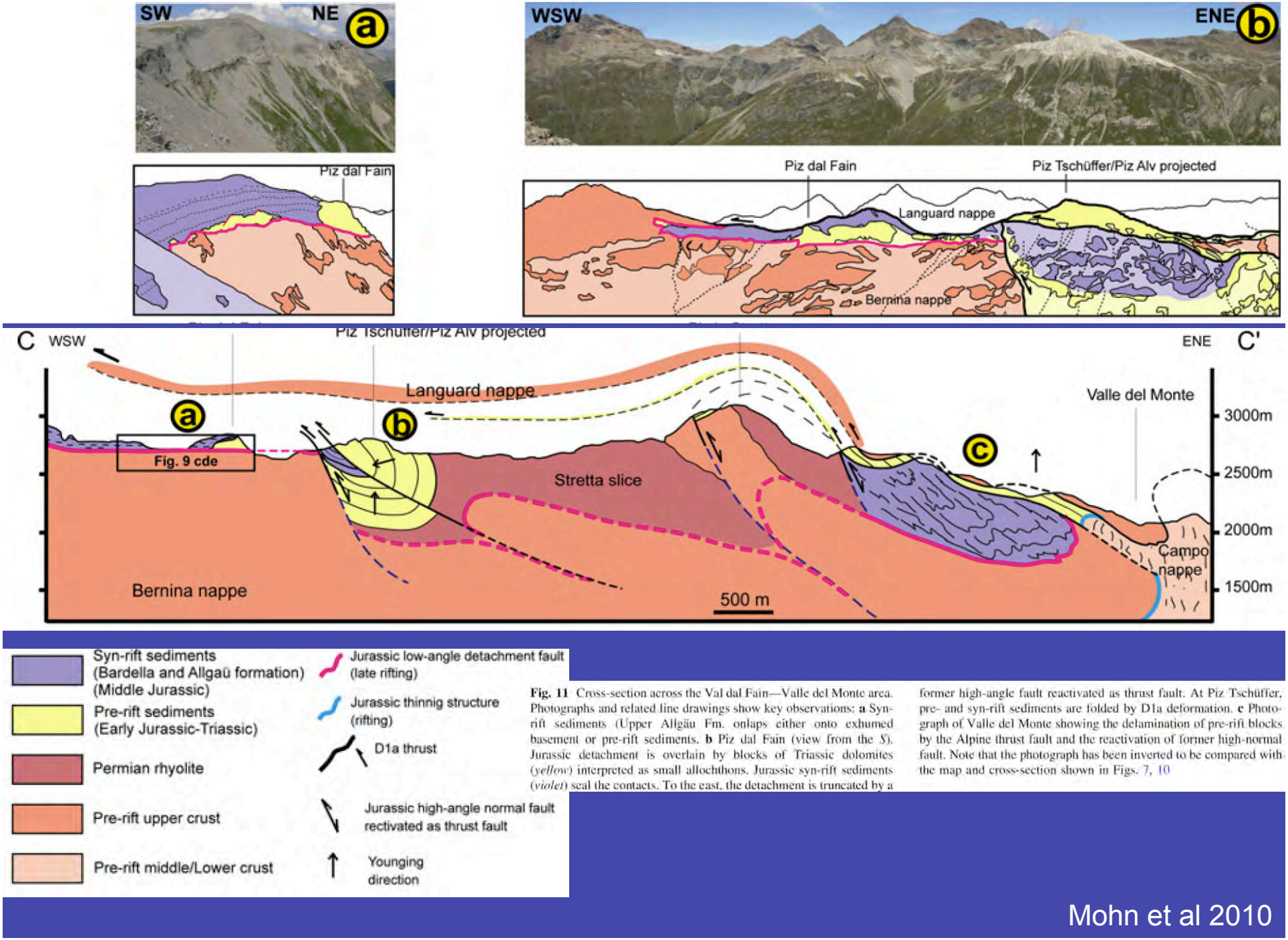

Fig. 11 Cross-section across the Val dal Fain—Valle del Monte area. Photographs and related line drawings show key observations: **a** Syn-rift sediments (Upper Allgäu Fm. onlaps either onto exhumed basement or pre-rift sediments. **b** Piz dal Fain (view from the *S*). Jurassic detachment is overlain by blocks of Triassic dolomites (*yellow*) interpreted as small allochthons. Jurassic syn-rift sediments (*violet*) seal the contacts. To the east, the detachment is truncated by a former high-angle fault reactivated as thrust fault. At Piz Tschüffer, pre- and syn-rift sediments are folded by D1a deformation. **c** Photograph of Valle del Monte showing the delamination of pre-rift blocks by the Alpine thrust fault and the reactivation of former high-normal fault. Note that the photograph has been inverted to be compared with the map and cross-section shown in Figs. 7, 10

Mohn et al 2010

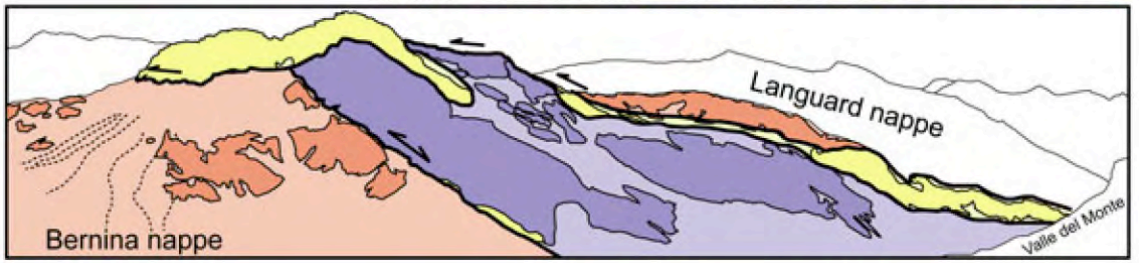

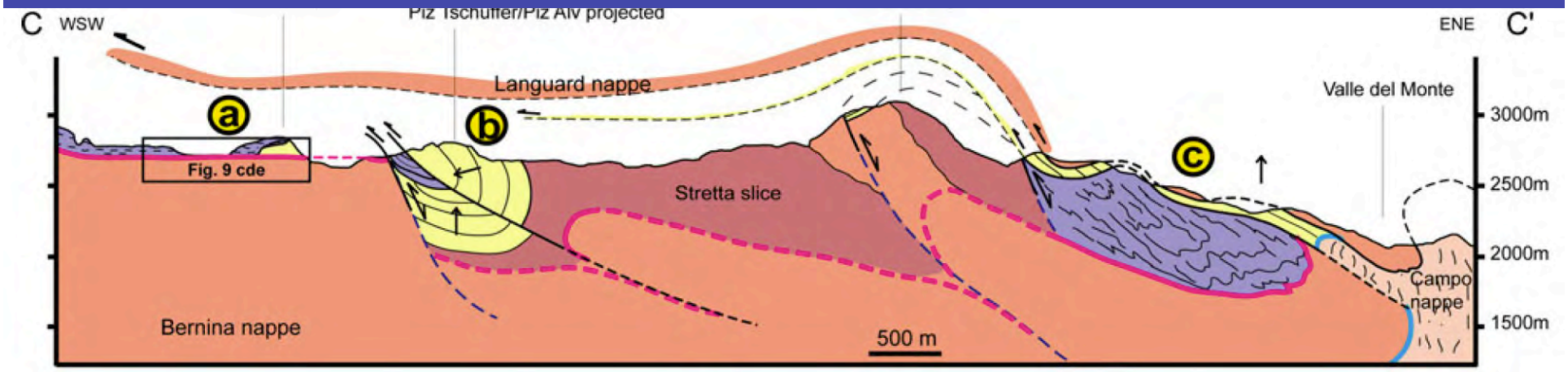

Syn-rift sediments (Bardella and Allgaü formation) (Middle Jurassic)

Pre-rift sediments (Early Jurassic-Triassic)

Permian rhyolite

Pre-rift upper crust

Pre-rift middle/Lower crust

Jurassic low-angle detachment fault (late rifting)

Jurassic thinnig structure (rifting)

D1a thrust

Jurassic high-angle normal fault rectivated as thrust fault

Younging direction

Fig. 11 Cross-section across the Val dal Fain—Valle del Monte area. Photographs and related line drawings show key observations: **a** Syn-rift sediments (Upper Allgäu Fm. onlaps either onto exhumed basement or pre-rift sediments. **b** Piz dal Fain (view from the *S*). Jurassic detachment is overlain by blocks of Triassic dolomites (*yellow*) interpreted as small allochthons. Jurassic syn-rift sediments (*violet*) seal the contacts. To the east, the detachment is truncated by a former high-angle fault reactivated as thrust fault. At Piz Tschüffer, pre- and syn-rift sediments are folded by D1a deformation. **c** Photograph of Valle del Monte showing the delamination of pre-rift blocks by the Alpine thrust fault and the reactivation of former high-normal fault. Note that the photograph has been inverted to be compared with the map and cross-section shown in Figs. 7, 10

Mohn et al 2010

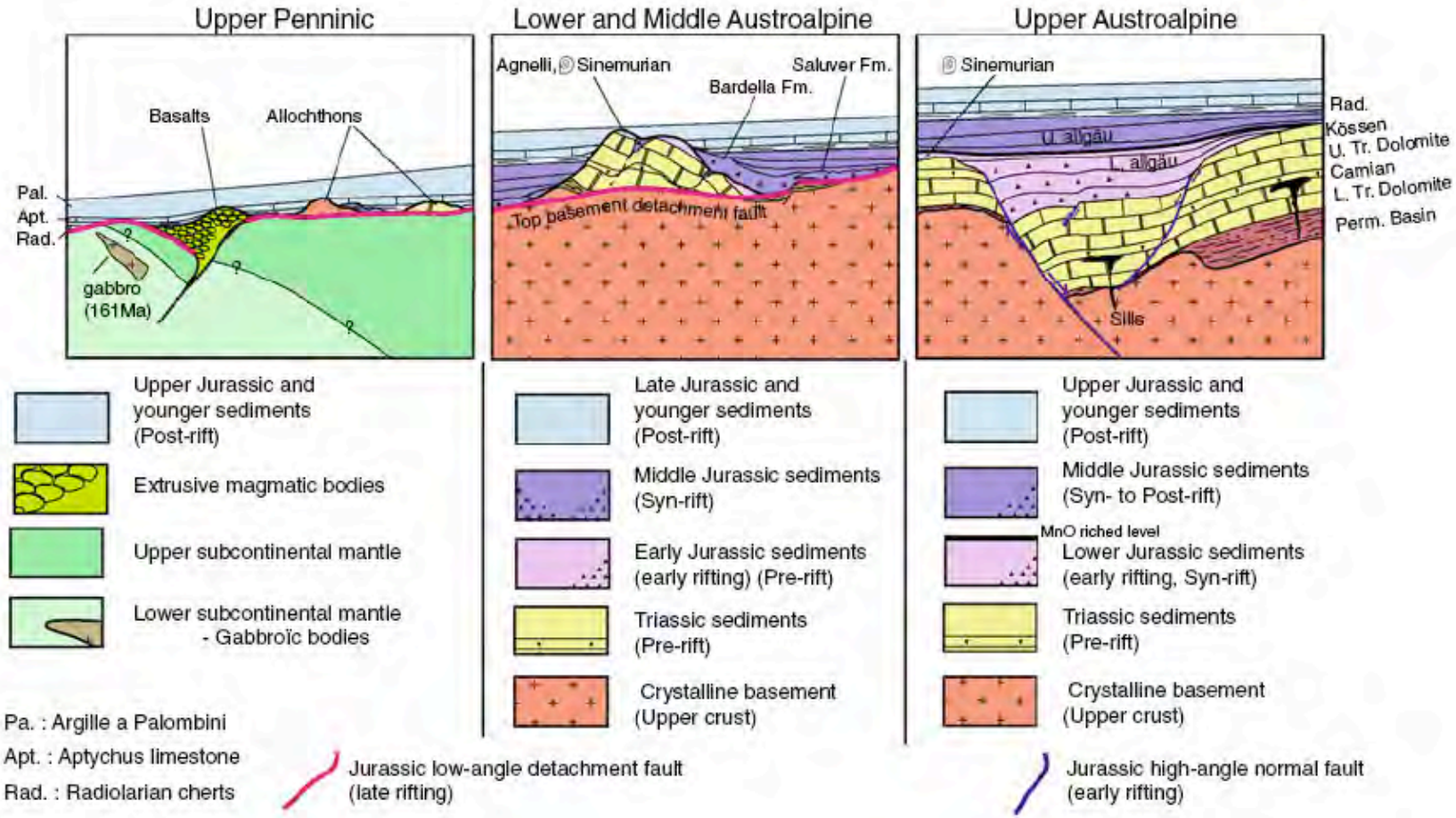

Fig. 5 Stratigraphic architecture of the Mesozoic sediments observed in the Austroalpine and Upper Penninic nappes in SE-Switzerland and N-Italy. Cartoons exemplify the observed stratigraphic and tectonic relationships observed in the UAA, MAA, LAA and Upper Penninic nappes

Mohn et al 2010

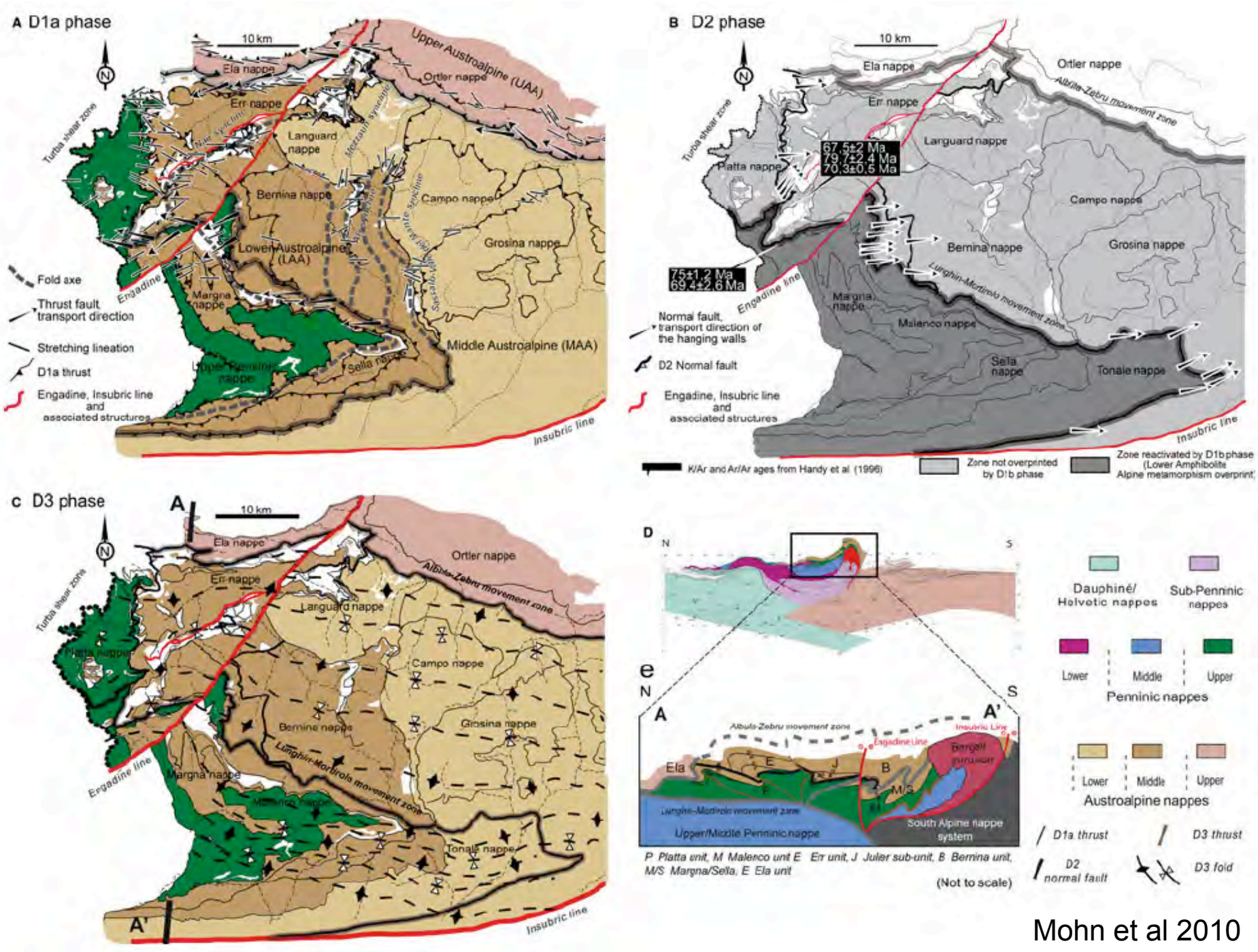

Mohn et al 2010

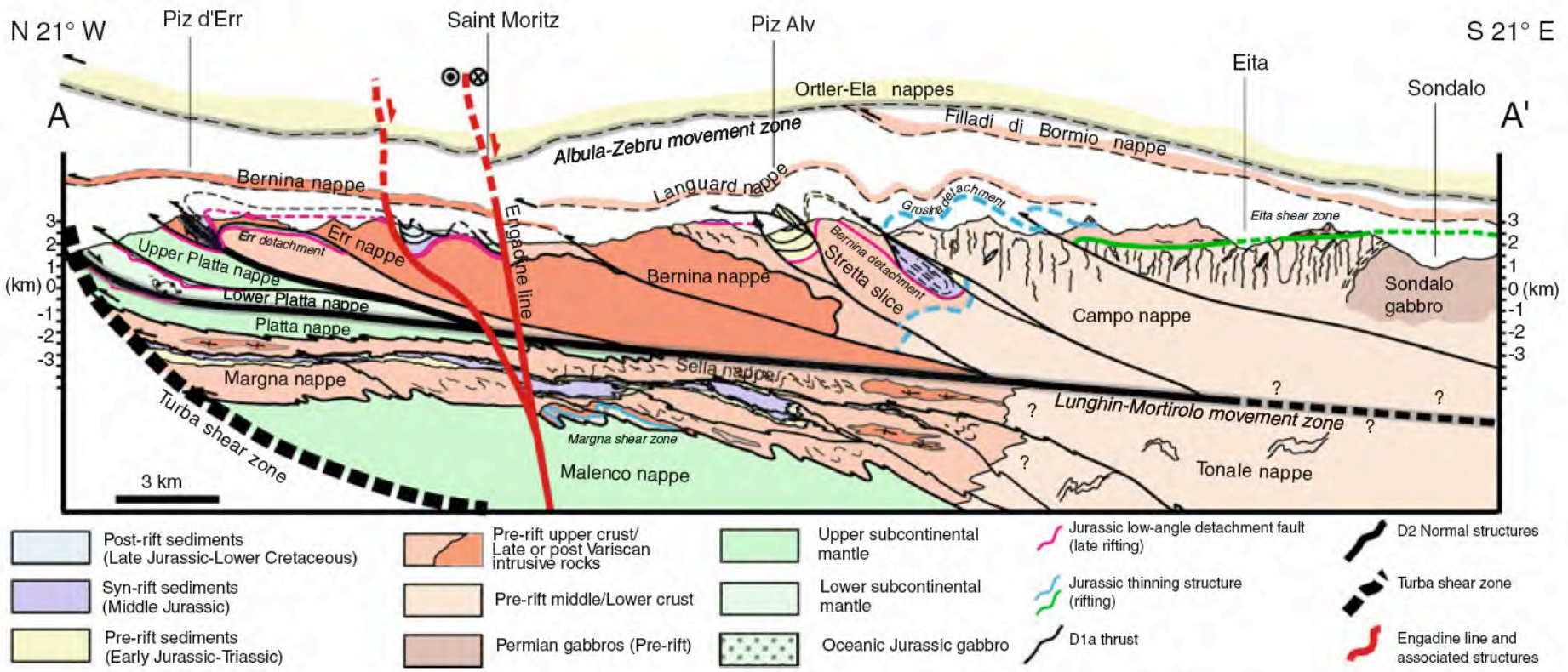

Fig. 7 Reconstructed Alpine section across the Upper Penninic and Austroalpine nappes in SE-Switzerland and N-Italy. Note the different styles of Alpine deformation in the hanging wall and footwall of the Lunghin—Mortirolo movement zone (for localization of the cross-section see Fig. 3)

Mohn et al 2010

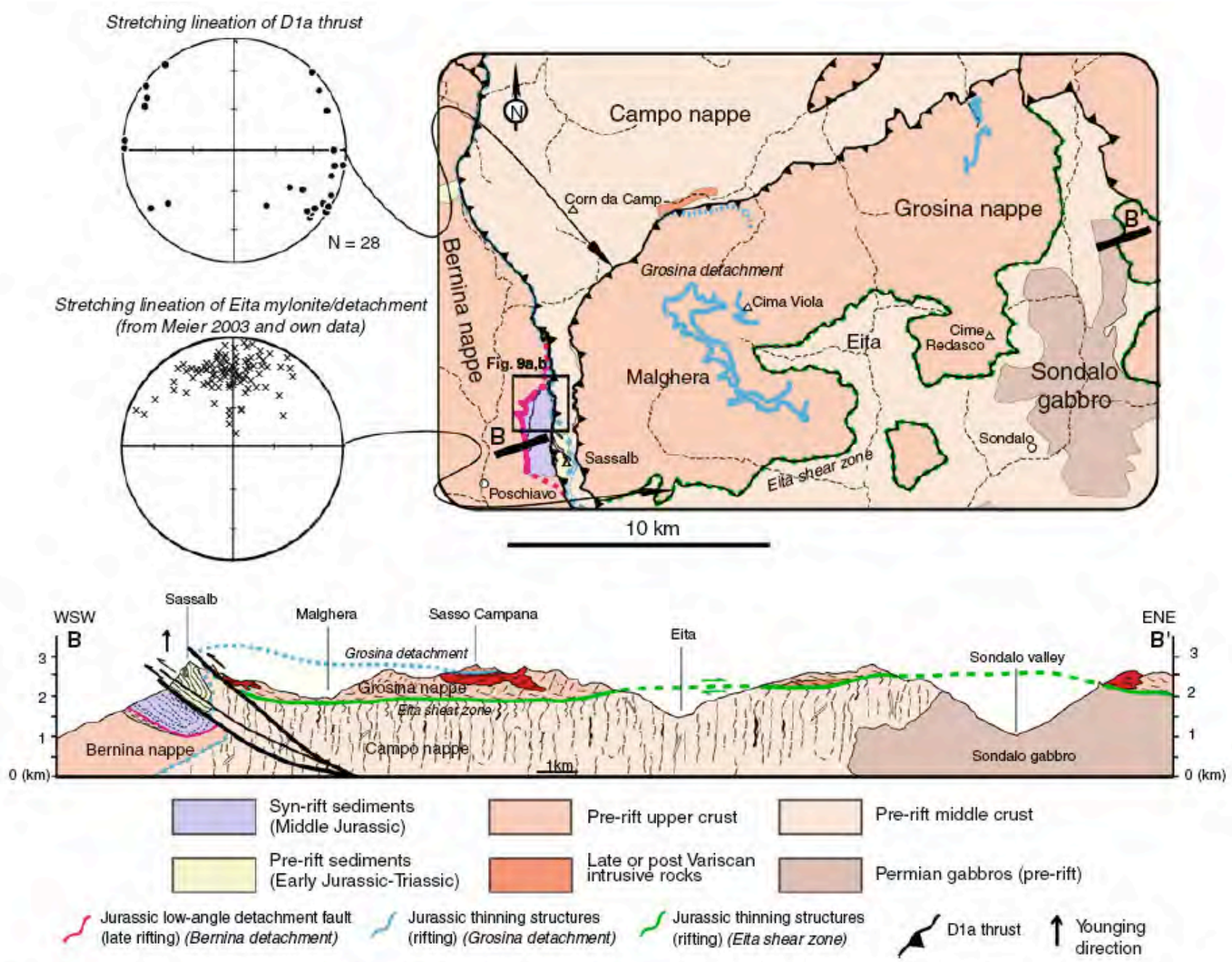

Fig. 8 Map and cross-section across the Sassalbo—Sondalo area showing the relationships between the Grosina, Campo and Bernina nappes. The stereographic projection is in equal area-lower hemisphere representation

Mohn et al 2010

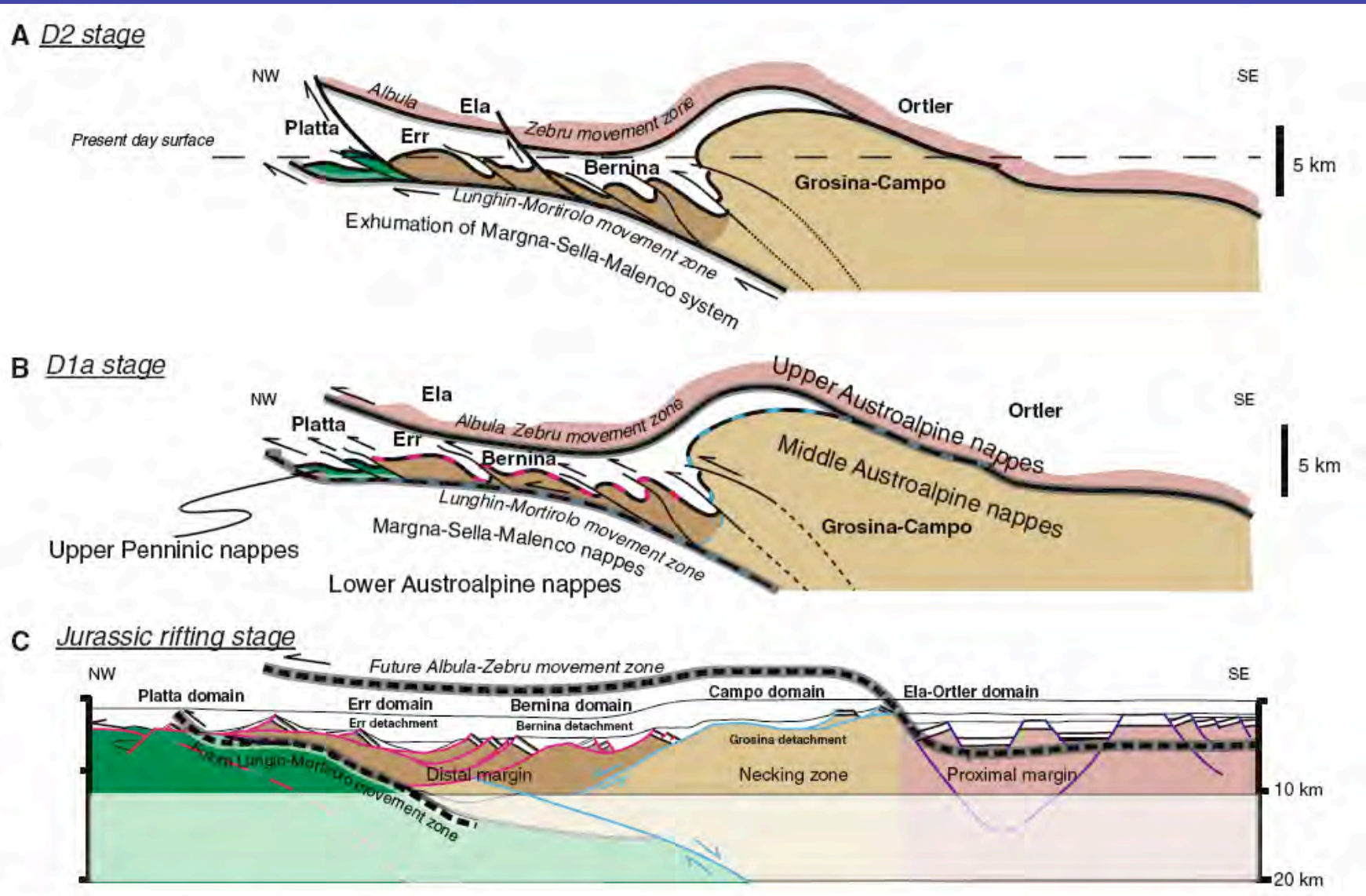

Fig. 12 Tectonic, large-scale restoration of the Austroalpine and Upper Penninic nappes in SE-Switzerland and N-Italy. **a** D2 Alpine phase, highlighting the importance of the Albula—Zebru and Lunghin—Mortirolo movement zones in accommodating most of the Alpine deformation. Note also that the relation between the Upper Penninic, Lower and Middle Austroalpine nappes inbetween the two movement zones is only moderately overprinted by Alpine deformation (for restoration see Fig. 13). **b** Reactivation of the former rift structures (on the scale of the margin) during the D1 Alpine phase. The Upper Austroalpine, Ela and Ortler nappes are thrust over Middle and Lower Austroalpine nappes. **c** Architecture of the Austroalpine (Adriatic) margin (modified from Mohn et al. 2010)

Mohn et al 2010

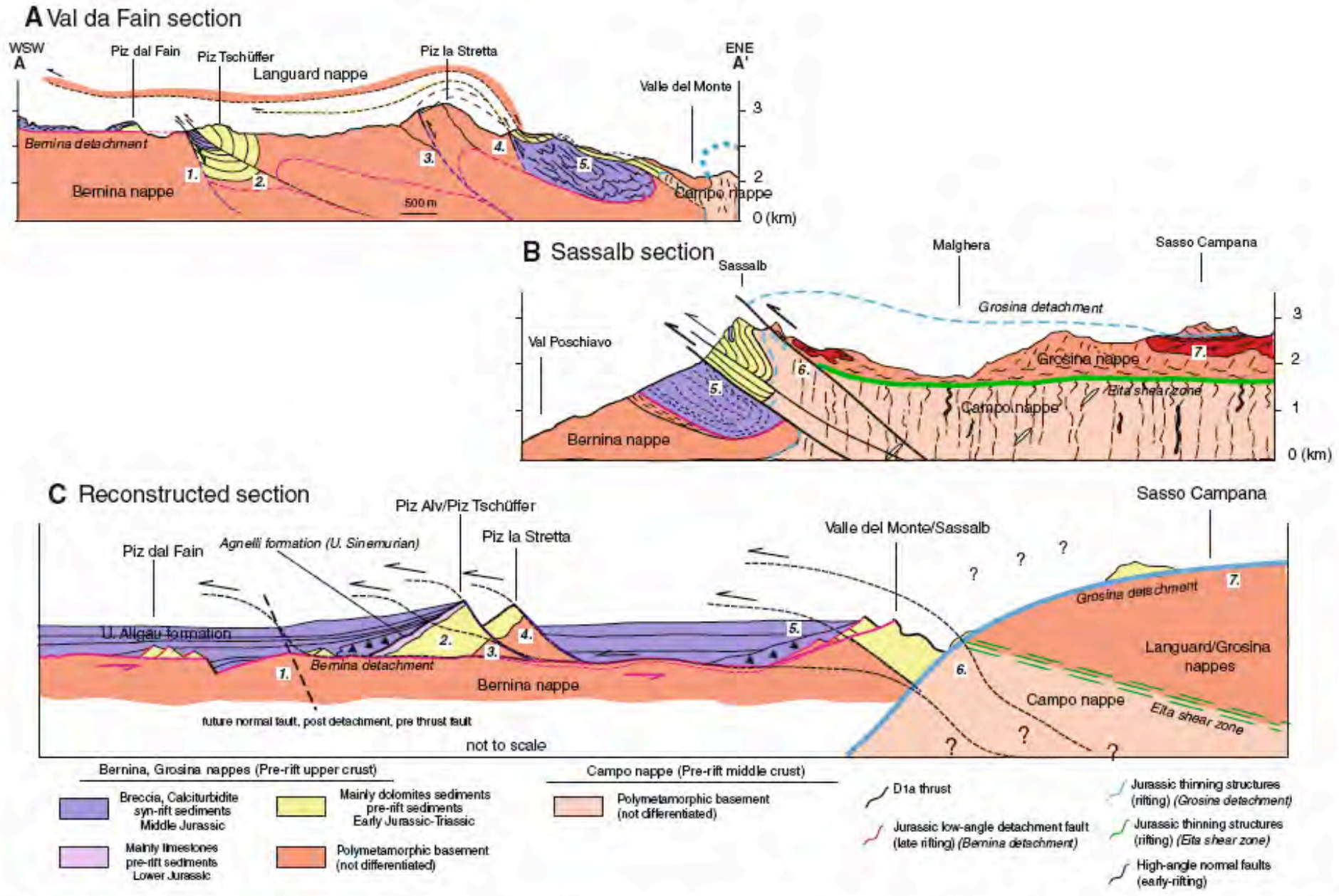

Fig. 13 Sections across a Val dal Fain and b Sassalbo—Val Grosina and c their restoration showing the importance of the rift inheritance during the subsequent Alpine tectonic overprint. Note that in many places the Alpine thrust faults reactivate former Jurassic detachment faults

Mohn et al 2010

Fig. 1 Geological map of the Val Bavona region (NW Ticino). AA': geological cross-section through the area of detailed study, shown on Fig. 10. Modified from Steck et al. (1999) and Berger and Mercolli (2006)

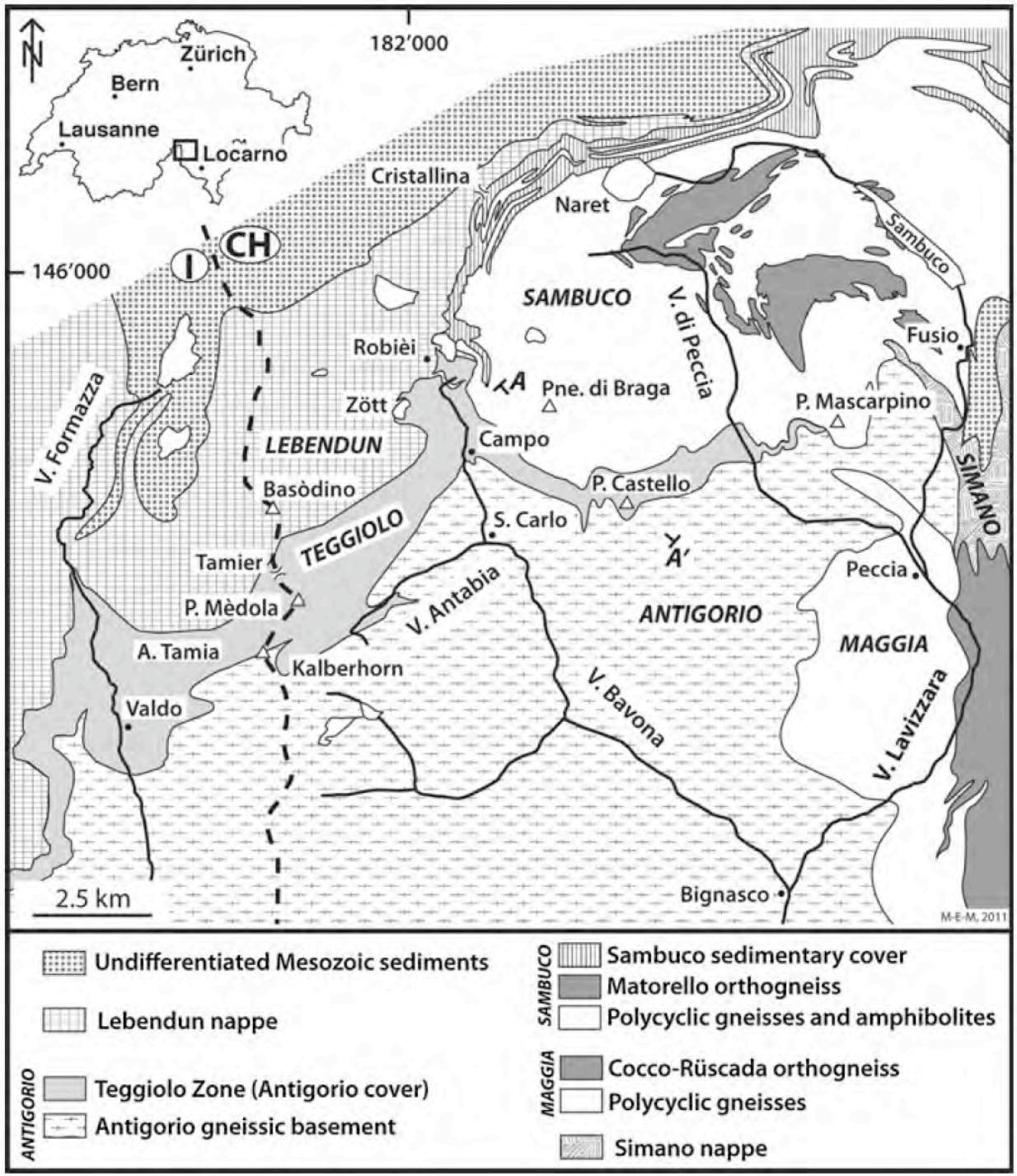

Metasci et al 2011

Fig. 2 Synthetic stratigraphic sections of the Teggiolo zone in the Val Bavona. The sedimentary cycles distinguished in the text are as follows: first cycle, Dolomite (Triassic); second cycle, Ri d'Antabia conglomerate, Sevinèra sandstone, Sevinèra marble, Vanis banded marble (Jurassic–Early Cretaceous); third cycle, Piano delle Creste sandstone, Mèdola quartzite (Late Cretaceous–Tertiary); fourth cycle, Robièi wildflysch (Tertiary)

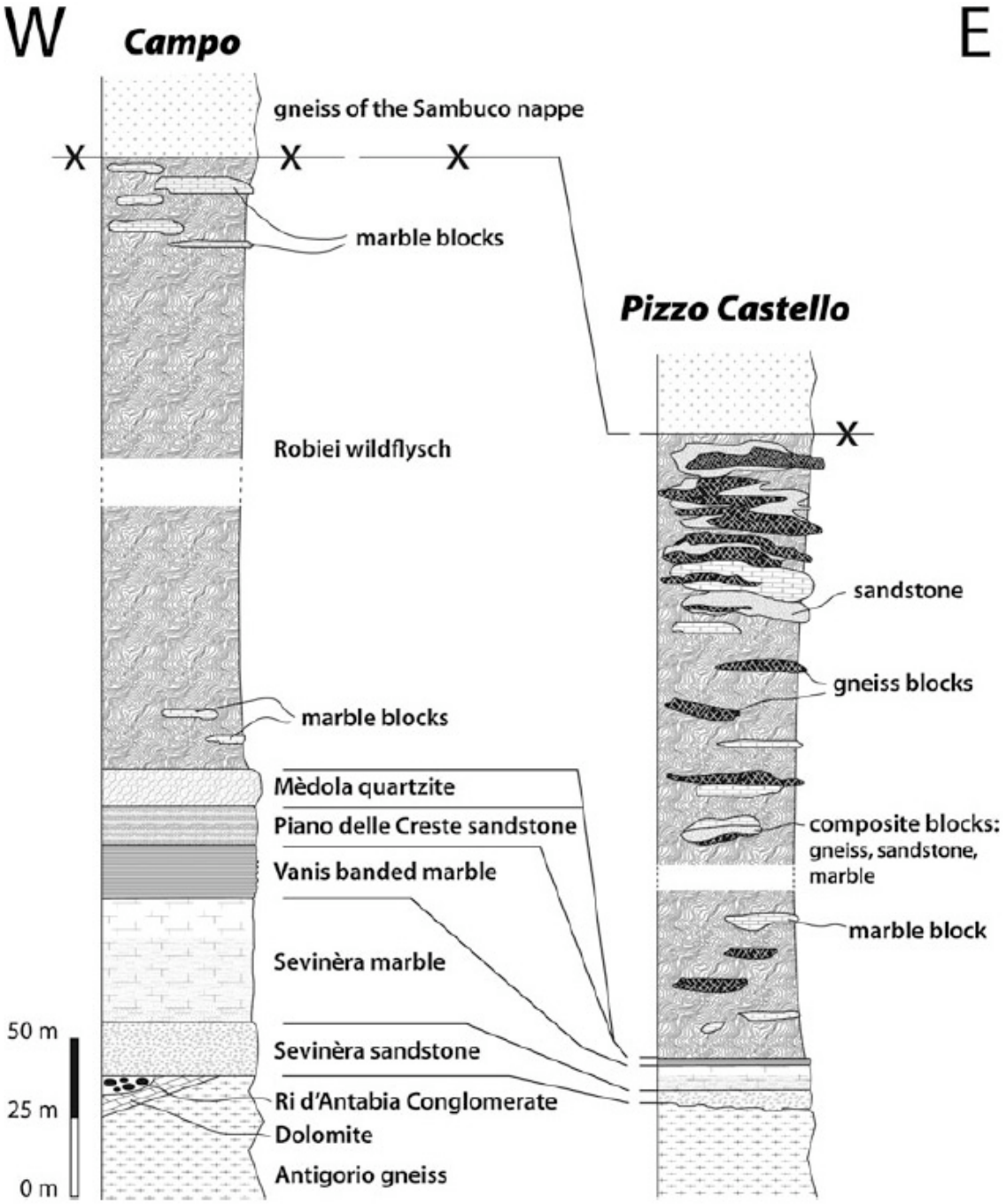

Metasci et al 2011

Fig. 5 Large block of marble in the Alpe Tamia–Campo wildflysch at Alpe Tamia. Smaller ones are also visible on the right. The crest is formed by the Lebendun gneiss thrusted over the Teggiolo zone. In the background: the Tamierpass

Metasci et al 2011

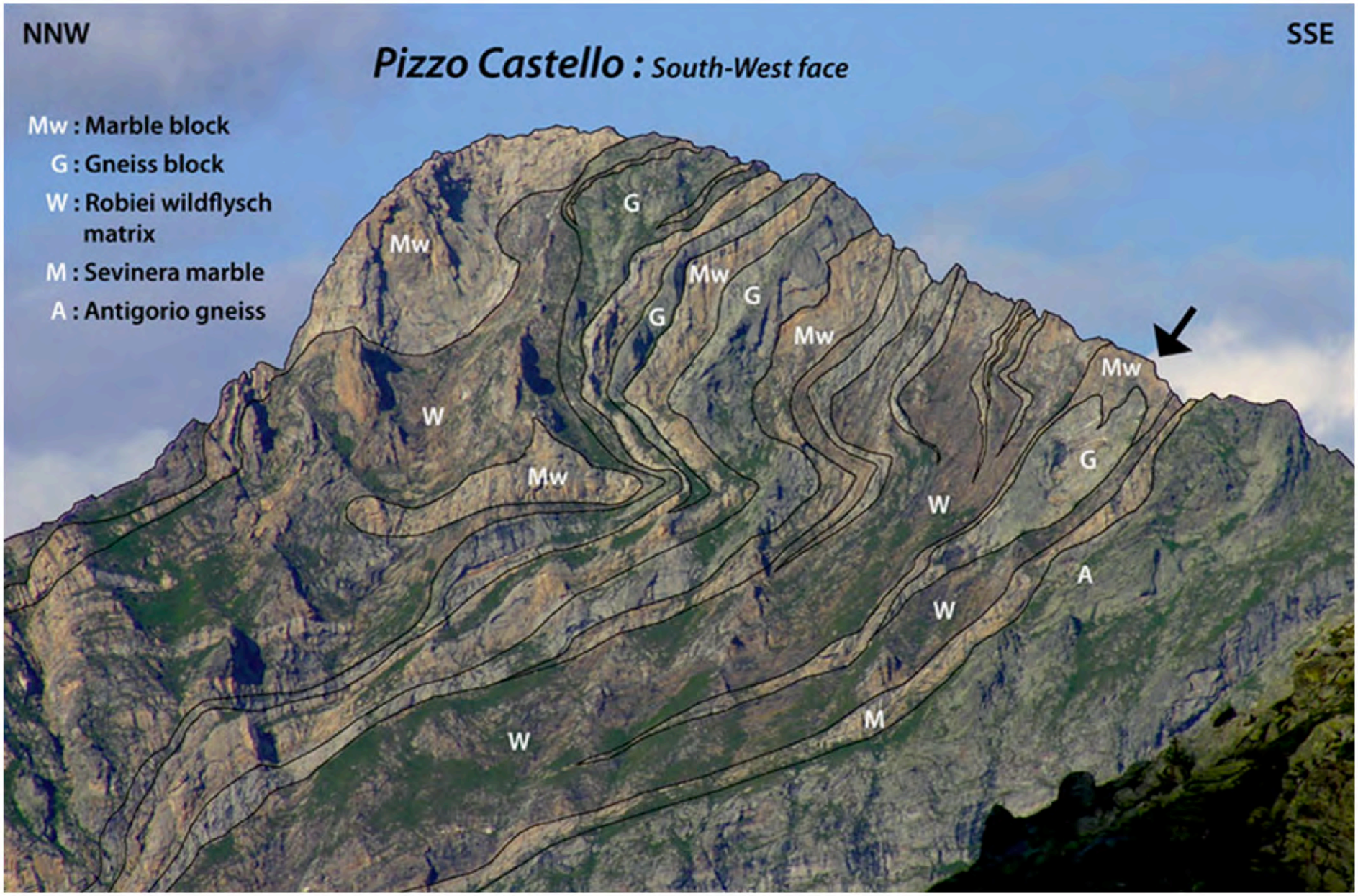

Fig. 7 Accumulation of very large blocks in the Pizzo Castello wildflysch. The arrow points to folds that existed before the formation of the blocks (height of cliff-face, ca. 300 m). Photo D. Bussien

Metasci et al 2011

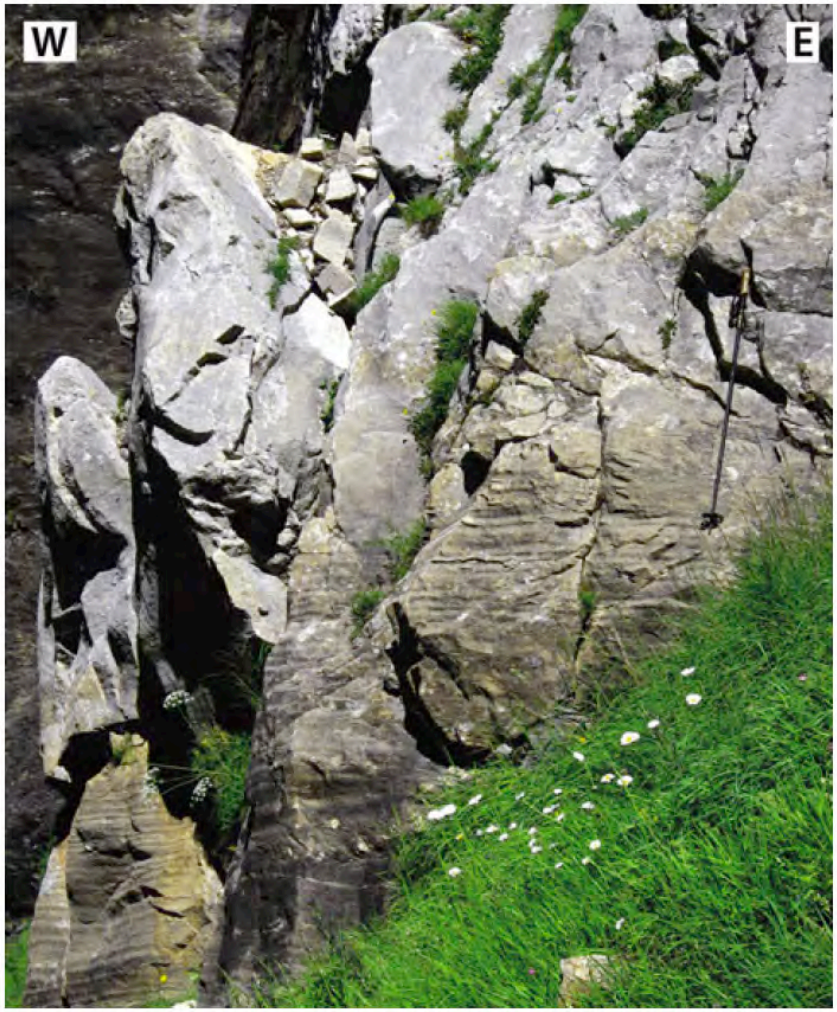

Fig. 3 The Sevinèra marble: gradual transition from the lower, banded "yellow" member to the upper, massive "white" member (ski-stick for scale, ca. 120 cm). Vanis ravine, ENE Campo (coord. 683.72/142.03)

Fig. 6 Block of gneiss embedded in the calcschist matrix of Tamier–Zött wildflysch. Smaller blocks are visible on the right. E of the Bavona river below the Cap. Basodino, Robièi (682.70/143.

Fig. 4 Small blocks of marble at the base of the Alpe Tamia–Campo wildflysch (hammer for scale, ca. 45 cm). Several marble pebbles dispersed in the calcschist matrix surround the main block. NW Campo (683.00/142.10)

Metasci et al 2011

Fig. 8 Elongated blocks of gneiss (*light grey*) and marble (*light yellowish*) in the brown calcschist matrix of the Pizzo Castello wildflysch. Corte di Là, W foot of Pizzo Castello (685.82/141.39)

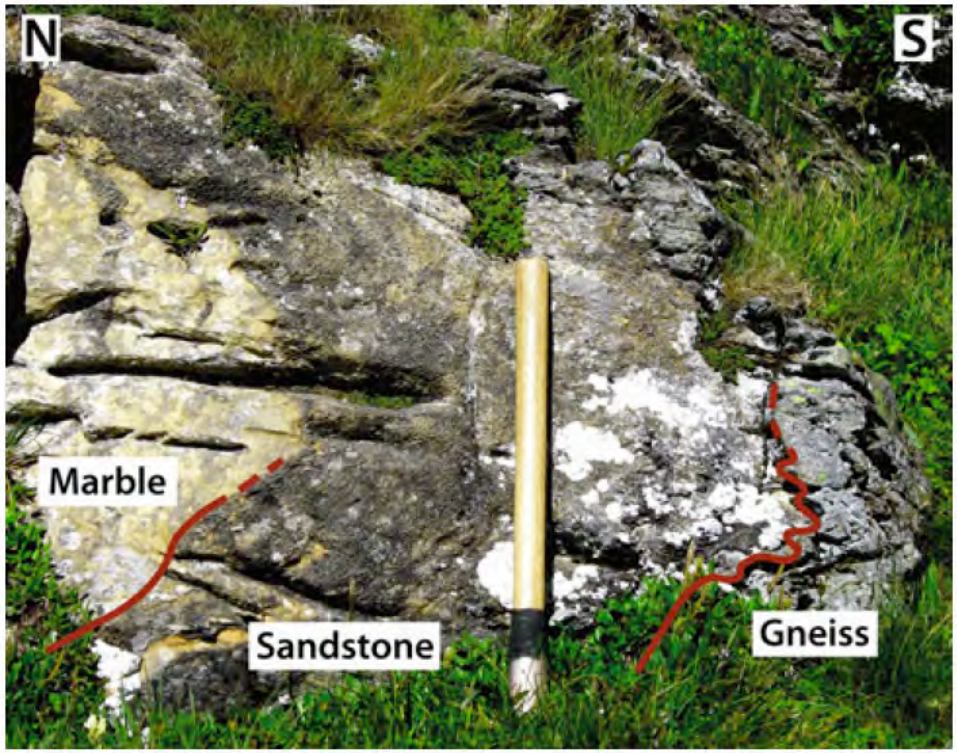

Fig. 9 Composite block of the Pizzo Castello wildflysch with the internal stratigraphic sequence marble/sandstone/gneiss (length of hammer shaft, ca. 60 cm). Alpe Serodano, 1 km NE Pizzo Castello (687.70/141.89)

Metasci et al 2011

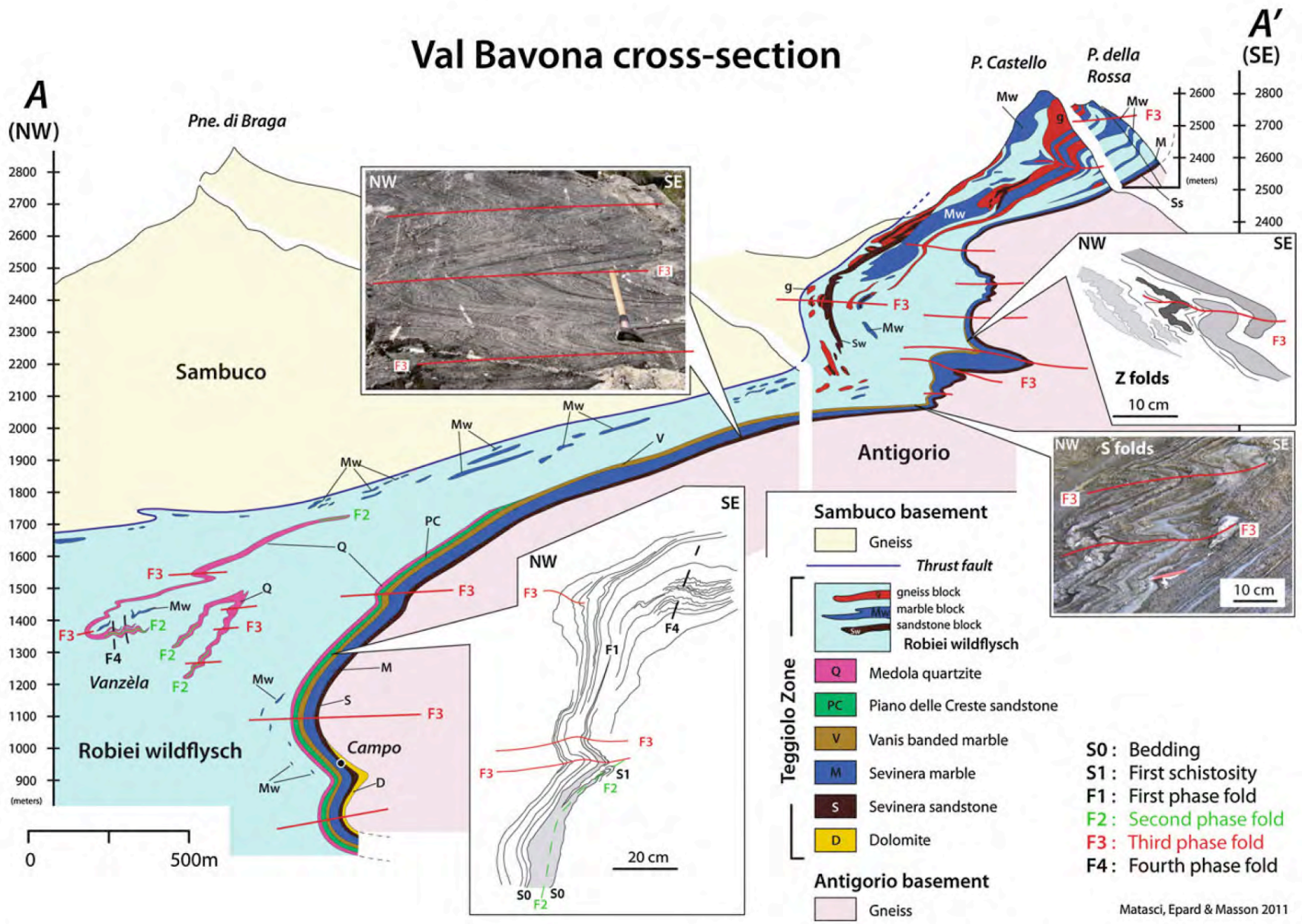

Fig. 10 Geological cross-section of the Antigorio nappe on the E bank of Val Bavona, showing the results of structural analysis in terms of four phases of ductile deformation, as described in the text (AA′ on Fig. 1)

Metasci et al 2011

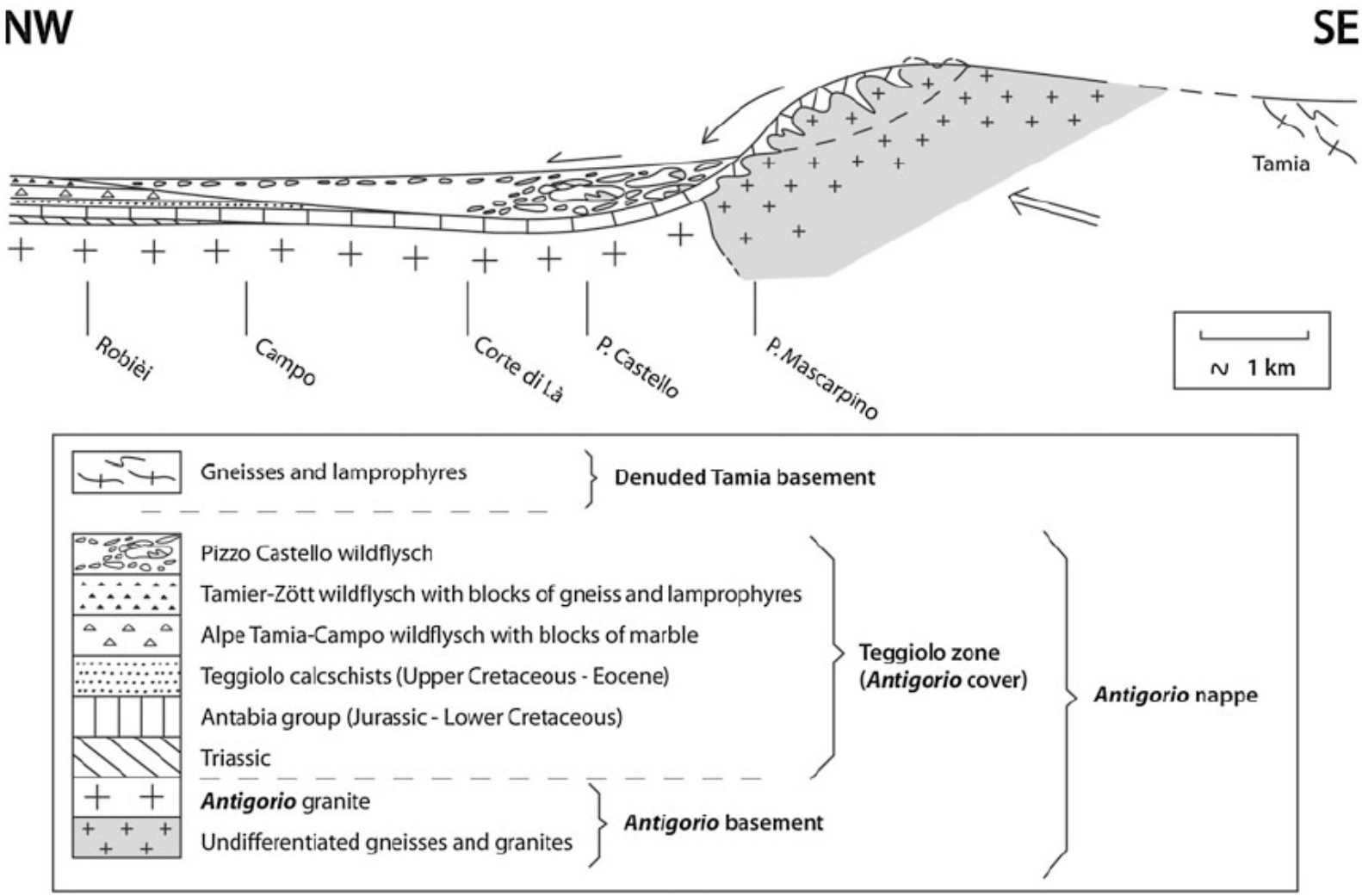

Fig. 12 Conceptual model of the Pizzo Castello wildflysch trough. The hypothetical Tamia land is inferred from the composition of the blocks of the Tamier–Zött and Alpe Tamia–Campo wildflyschs (see text). The *arrows* represent, from right to left, the "orogenic push", the collapse of the folded Pizzo Castello blocks, and their sliding on the bottom of the sea

Metasci et al 2011

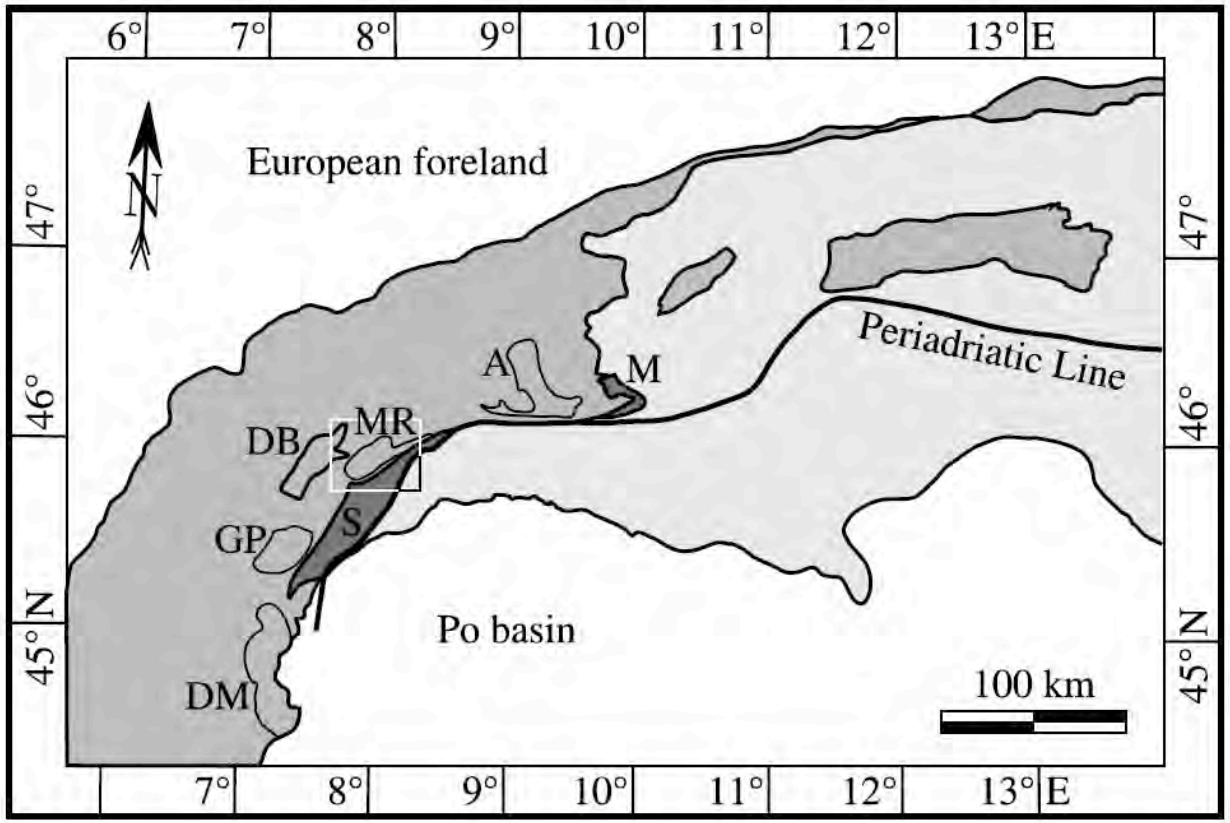

Figure 1. Tectonic sketch map of the Alps, showing the position of the Monte Rosa nappe (MR) and other continental high-pressure nappes of the Penninic zone: Adula (A), Gran Paradiso (GP), Dora-Maira (DM). DB, Dent Blanche nappe; M, Margna nappe; S, Sesia nappe. Rectangle indicates map area of Figure 3.

Plueger et al 2005

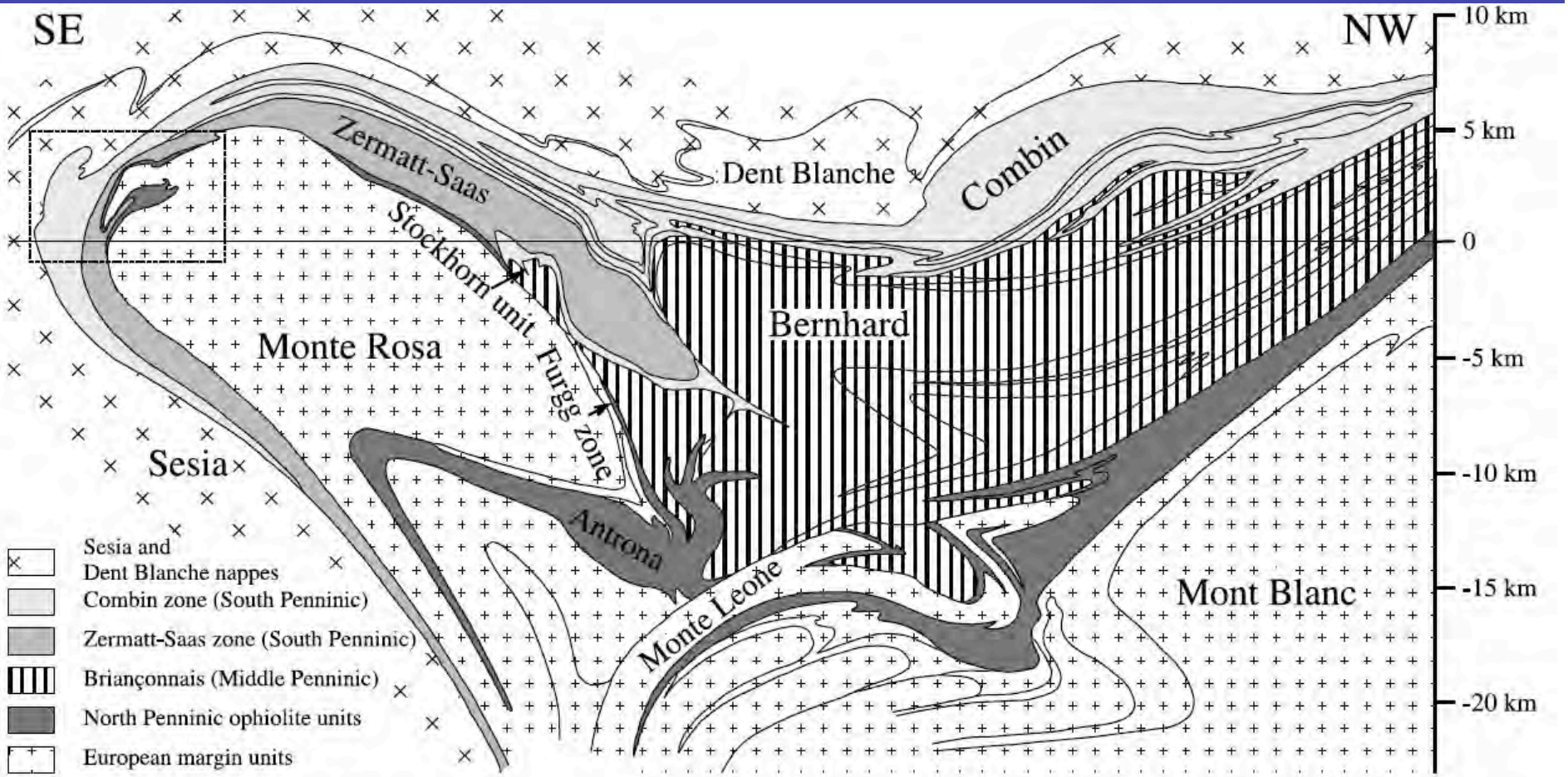

Figure 2. Cross section through the western Swiss-Italian Alps, modified after *Escher et al.* [1993]. The units are combined according to their paleogeographic origins proposed in this paper. Thin black lines within tectonic units are second-order nappe boundaries and lithological boundaries which are shown in order to highlight the internal structures. Dashed rectangle indicates approximate location of the study area.

Plueger et al 2005

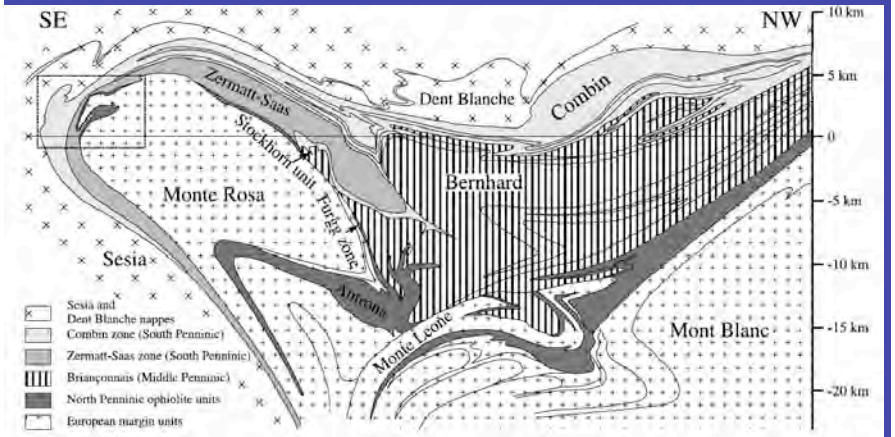

Figure 2. Cross section through the western Swiss-Italian Alps, modified after *Escher et al.* [1993]. The units are combined according to their paleogeographic origins proposed in this paper. Thin black lines within tectonic units are second-order nappe boundaries and lithological boundaries which are shown in order to highlight the internal structures. Dashed rectangle indicates approximate location of the study area.

Plueger et al 2005

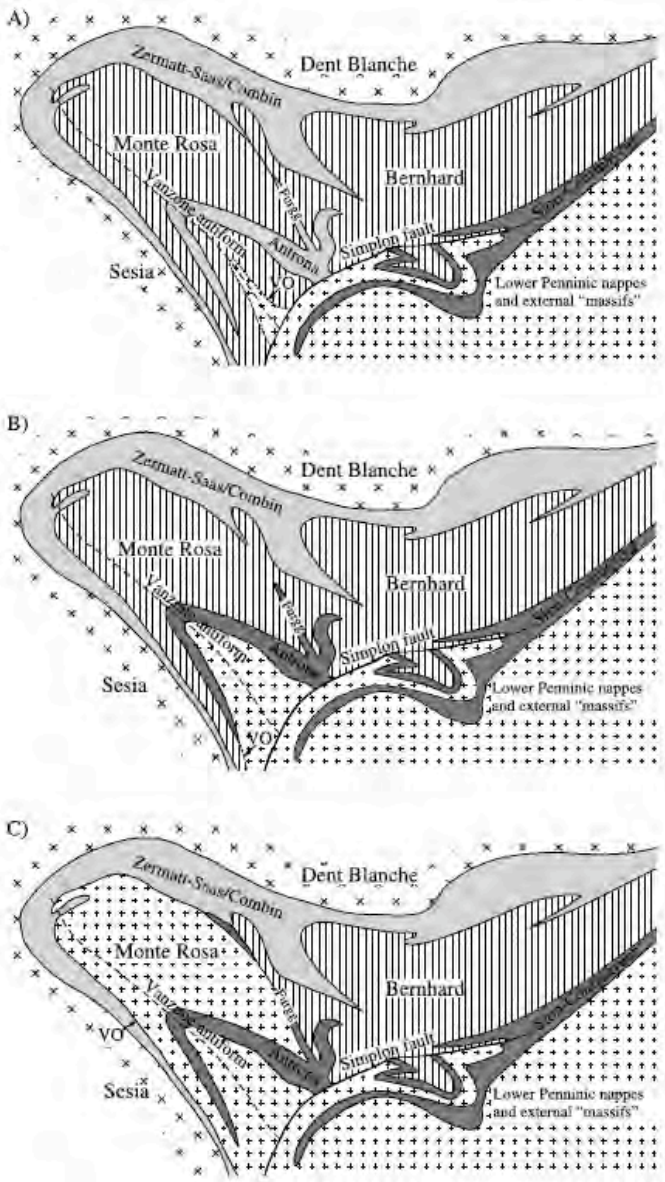

Figure 5. Schematic cross sections illustrating different paleogeographic restorations of the Penninic nappes. Patterns are as in Figure 2, with the only difference that the Zermatt-Saas and Combin zones are merged (light grey). VO, suture of the Valais (North Penninic) ocean. (a) Model after *Escher et al.* [1993]. All the ophiolites above the Monte Rosa nappe are of South Penninic origin. The Antrona zone is a complex synform branching off from the Zermatt-Saas zone through the Furgg zone. (b) Model after *Keller and Schmid* [2001]. The Antrona unit is part of the Valais ocean and lying below the Monte Rosa nappe. Monte Rosa and Bernhard nappes are not separated by the Furgg zone. (c) Interpretation of *Froitzheim* [2001]. The North Penninic ocean is represented by the Antrona zone but rooted south of the Monte Rosa nappe. The Antrona zone is again interpreted as a complex synform.

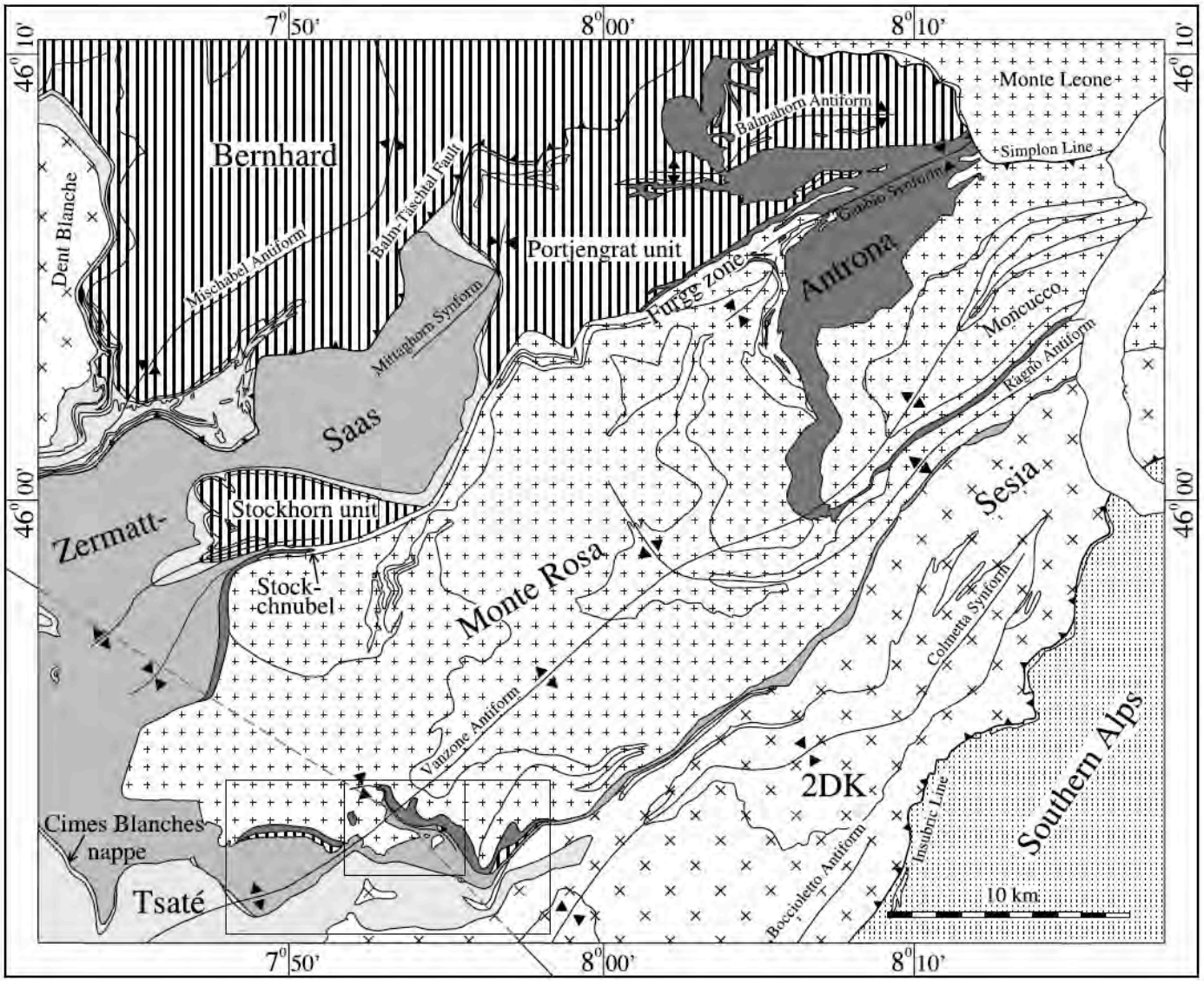

Figure 3. Simplified tectonic map of the Monte Rosa nappe and adjacent units, modified after *Steck et al.* [1999]. Patterns are as in Figure 2. The large and small rectangles correspond to the mapped areas of Figures 6 and 7, respectively. The dashed line marks the trace of the cross section shown in Figure 2. 2DK, seconda zona dioritico-kinzigitica (second diorite-kinzigite zone).

Plueger et al 2005

Figure 10. Stolemberg seen from the west. The gneissic rock slice of the Stolemberg unit is separated from the Monte Rosa paragneisses by serpentinite and some amphibolite of the Balma unit. The Zermatt-Saas amphibolites rest on top of the mountain. The structural position is in the normal-lying upper limb of the Cimalegna fold.

Plueger et al 2005

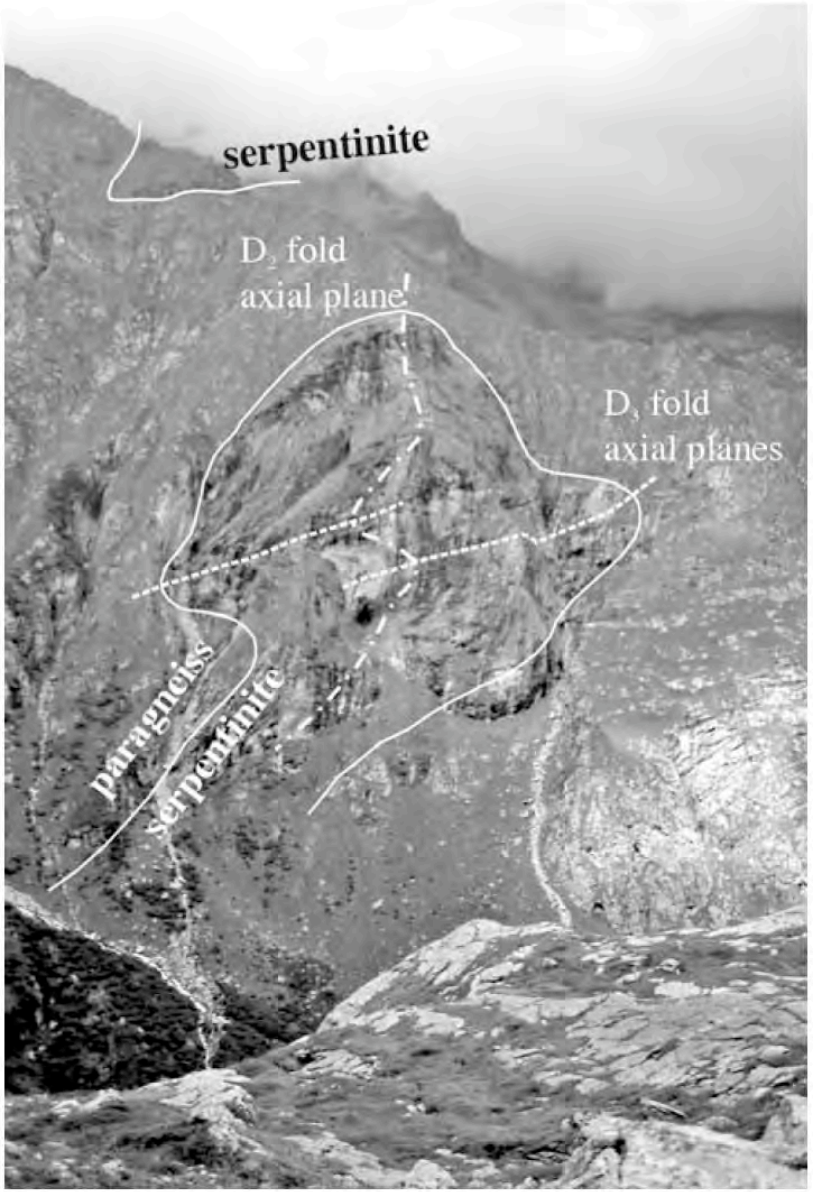

Figure 16. D_2 antiform with serpentinite of the Balma unit in its core (lower Malfatta fold) east of the Malfatta mountain seen from southeast. In this area the D_2 fold axis trends roughly north-south due to its reorientation by D_3 folds. The D_2 fold axial plane is bent by parasitic folds of the D_3 Molera fold.

Plueger et al 2005

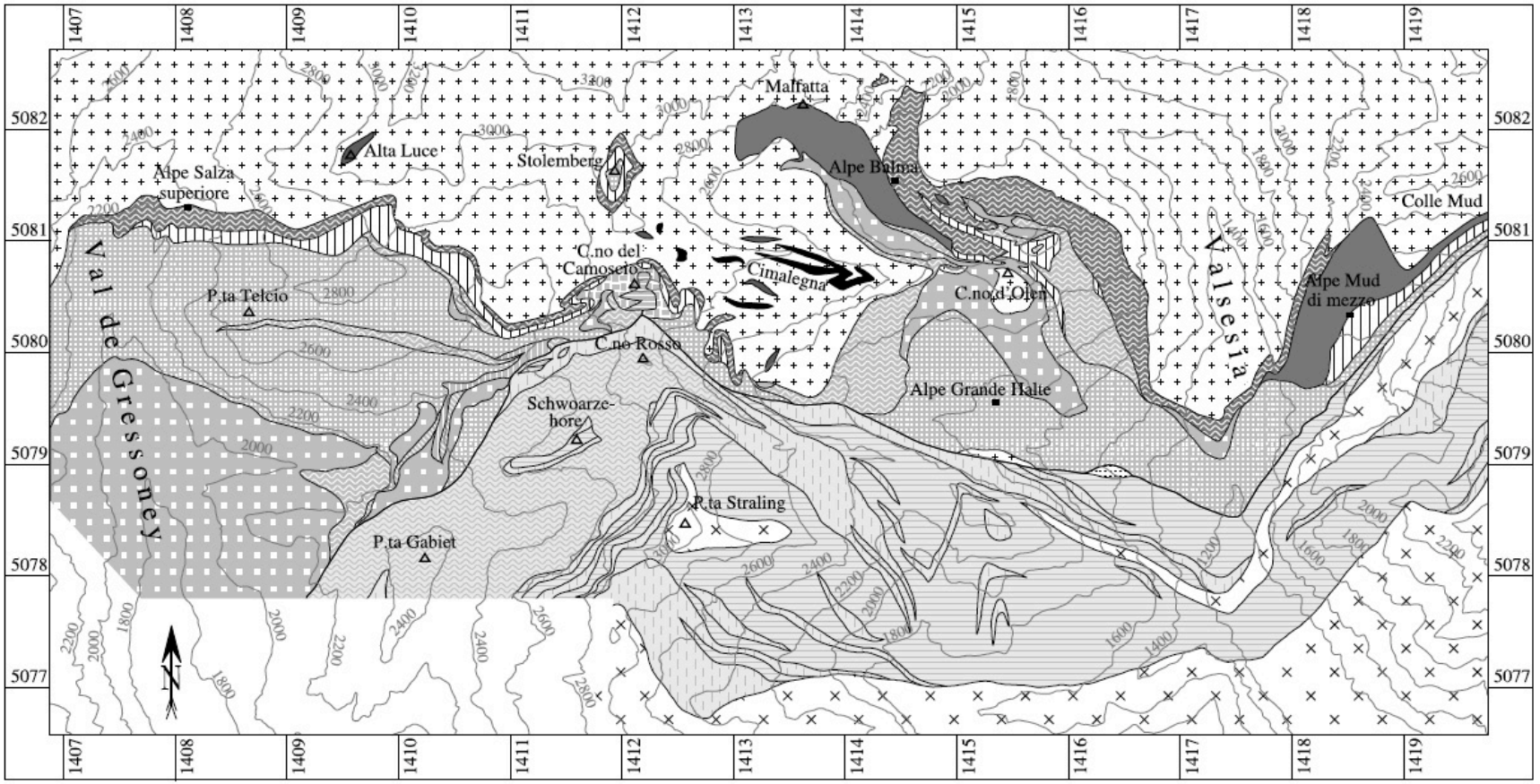

Sesia-Dent Blanche nappe
- Gneiss, metapelite, metabasite

Tsaté nappe
- Calcschist
- Greenschist
- Serpentinite
- not subdivided

Cimes Blanches nappe
- Quartzite, arkose

Zermatt-Saas zone
- Greenschist breccia
- Mélange
- Metagreywacke
- Calcschist

Zermatt-Saas zone
- Metagabbro
- Amphibolite
- Eclogite
- Serpentinite

Stolemberg unit
- Paragneiss

Balma unit
- Eclogite
- Amphibolite
- Serpentinite

Monte Rosa nappe
- Amphibolite
- Eclogite
- Paragneiss, orthogneiss

Figure 6. Geologic map of the upper Sesia and Gressoney valleys, showing all occurrences of Stolemberg and Balma unit rocks at the southern side of the Monte Rosa nappe. The internal arrangement of the Tsaté nappe in upper Valsesia is modified after *Mattirolo et al.* [1912, 1927]. Kilometric coordinates in the frame refer to the Italian Gauss-Boaga grid.

Plueger et al 2005

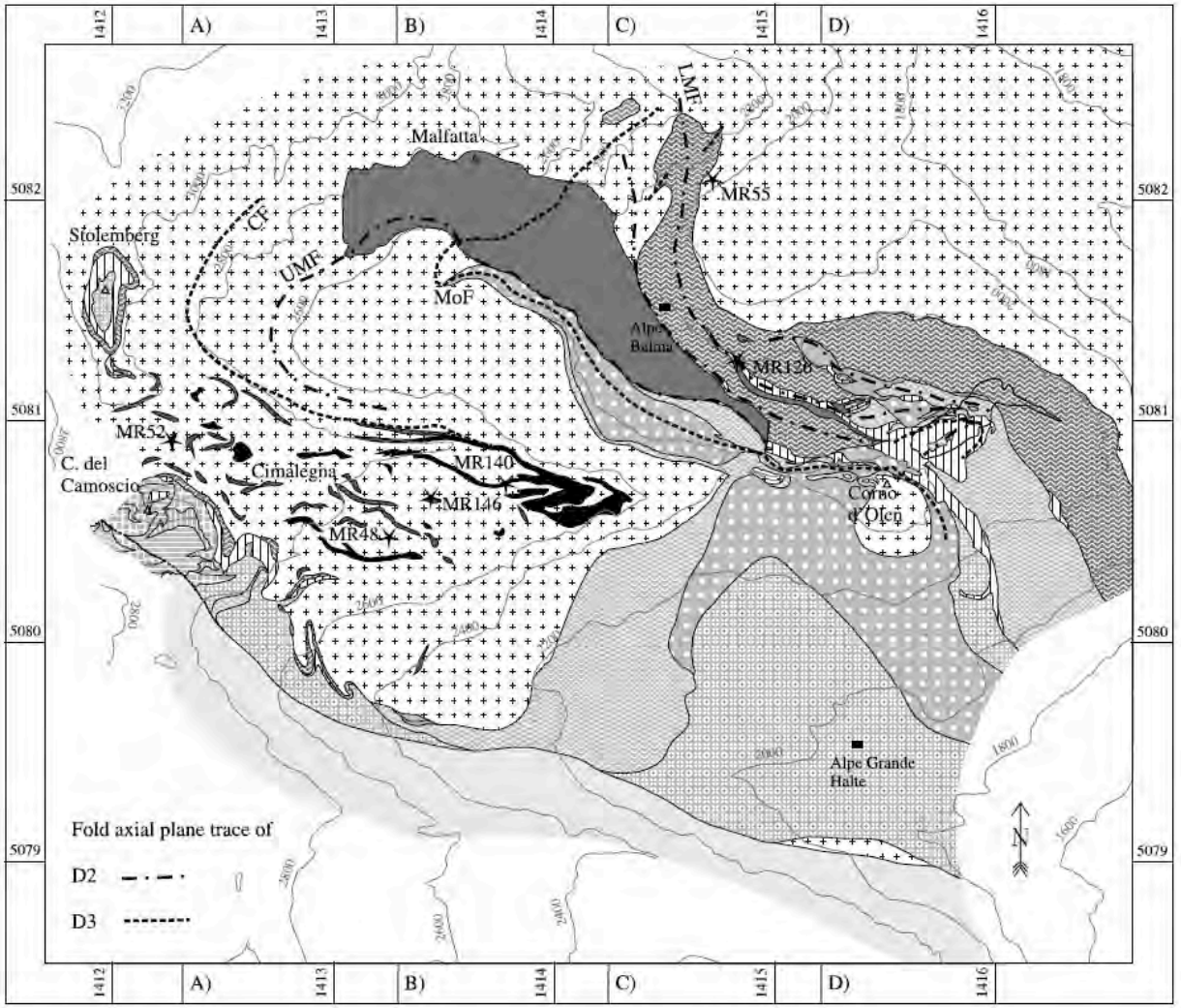

Figure 7. Geologic map of the Vallone delle Pisse (to the north) and Valle d'Olen (to the south) on the western side of the upper Sesia valley. The patterns are the same as in Figure 6. The western margin of the mapped area is the ridge between Gressoney valley and Sesia valley with the summits of Stolemberg and Corno del Camoscio. From the latter toward east extends the Cimalegna where amphibolitic and eclogitic lenses within Monte Rosa paragneiss have been mapped to better visualize the structures. The Corno d'Olen is a paragneiss klippe separated from the Cimalegna by a small topographic depression. The dashed lines are the axial traces of the southward closing D_3 Cimalegna fold (CF) and its underlying, northward closing counterpart (Molera fold, MoF). The latter bends two older folds (D_2), one with eclogite in its core (upper Malfatta fold, UMF) in the southern slopes of the mountain Malfatta and one with serpentinite further east (lower Malfatta fold, LMF), into the lower limb of the Cimalegna fold and thus strongly reorients their fold axes and axial planes. Stars mark sample locations for neutron texture studies. The grey lines within the frame give the traces of the cross sections in Figure 8. Kilometric coordinates in the frame refer to the Italian Gauss-Boaga grid.

Plueger
et al 2005

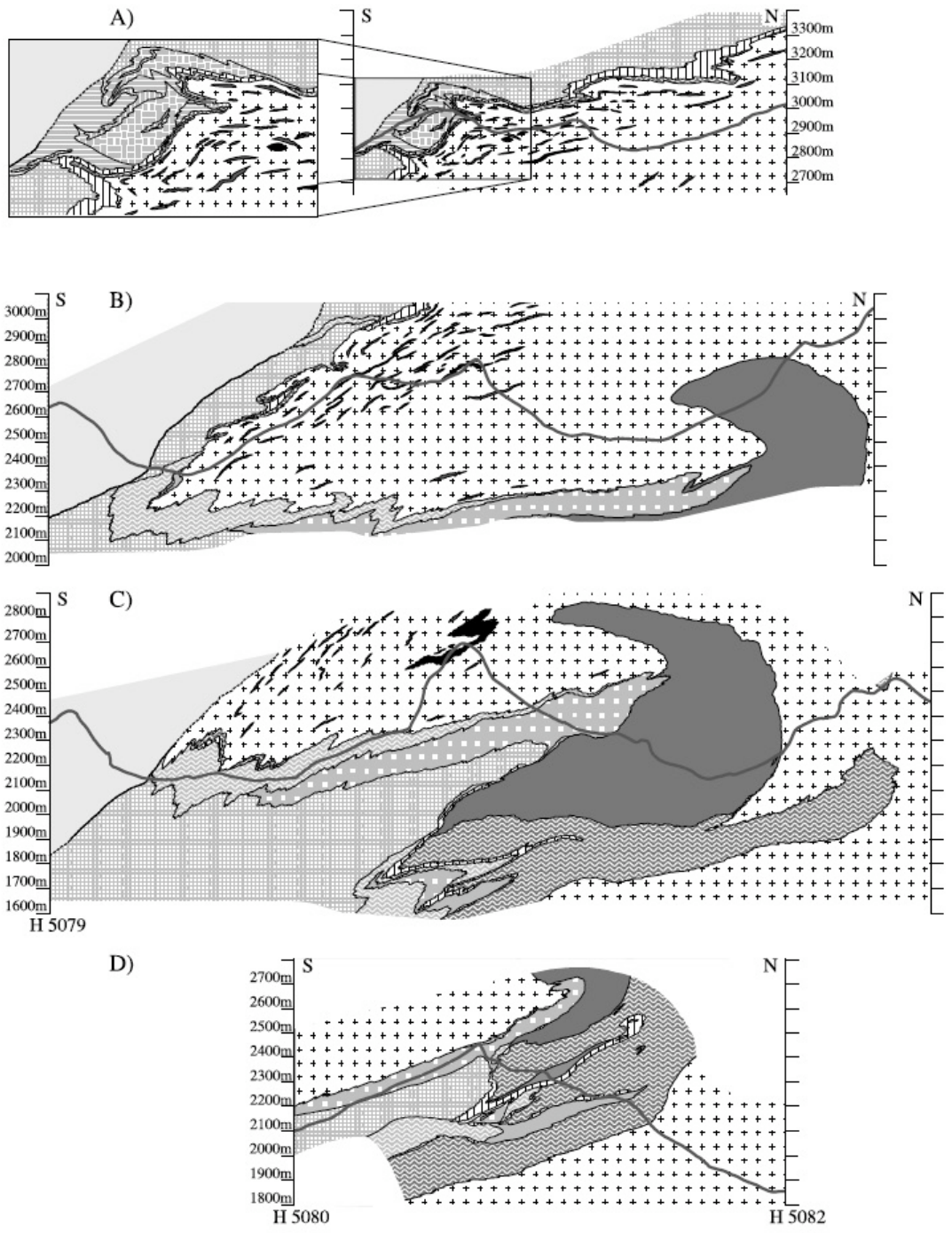

Figure 8

Plueger
et al 2005

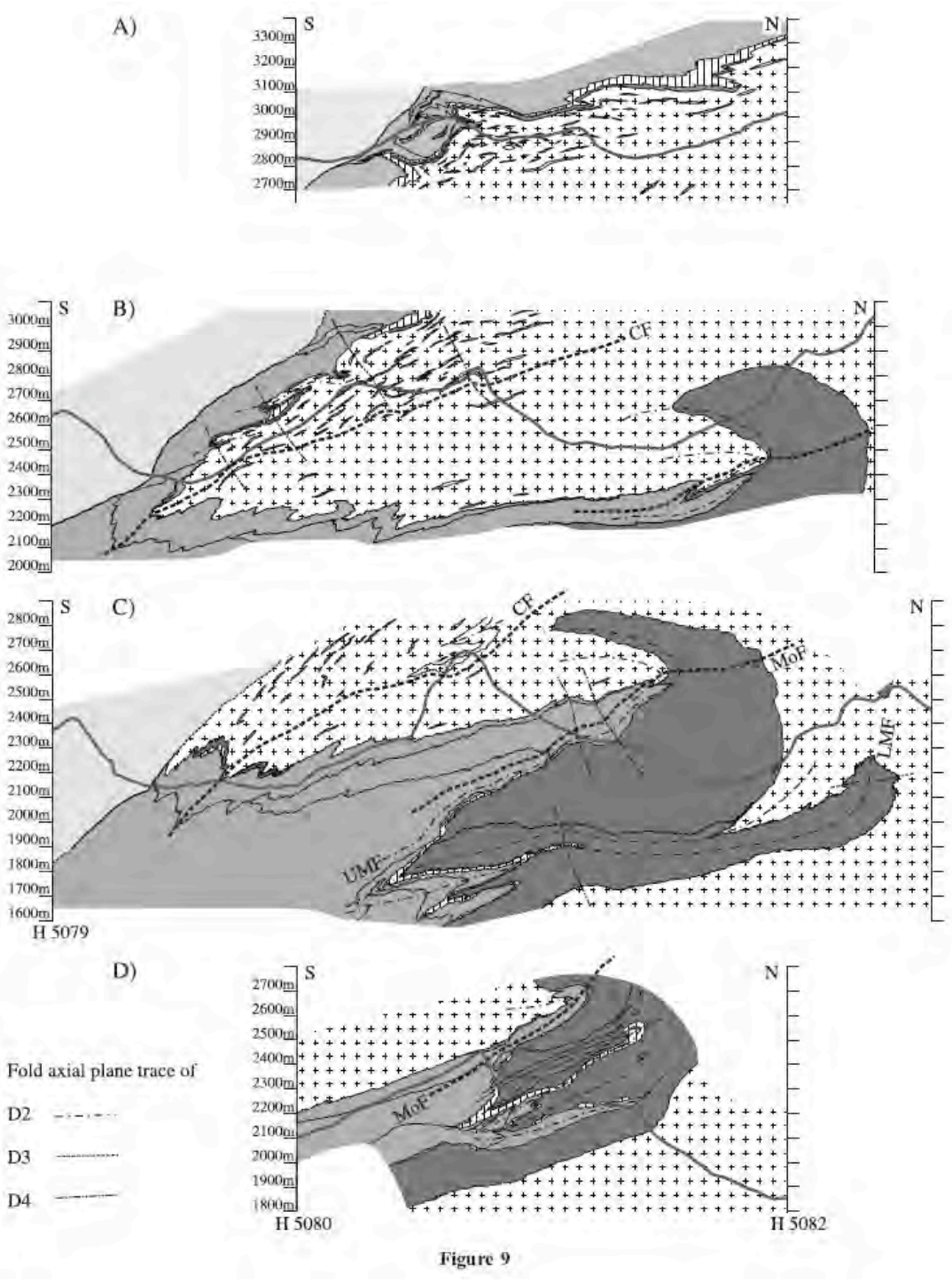

Figure 9

Plueger
et al 2005

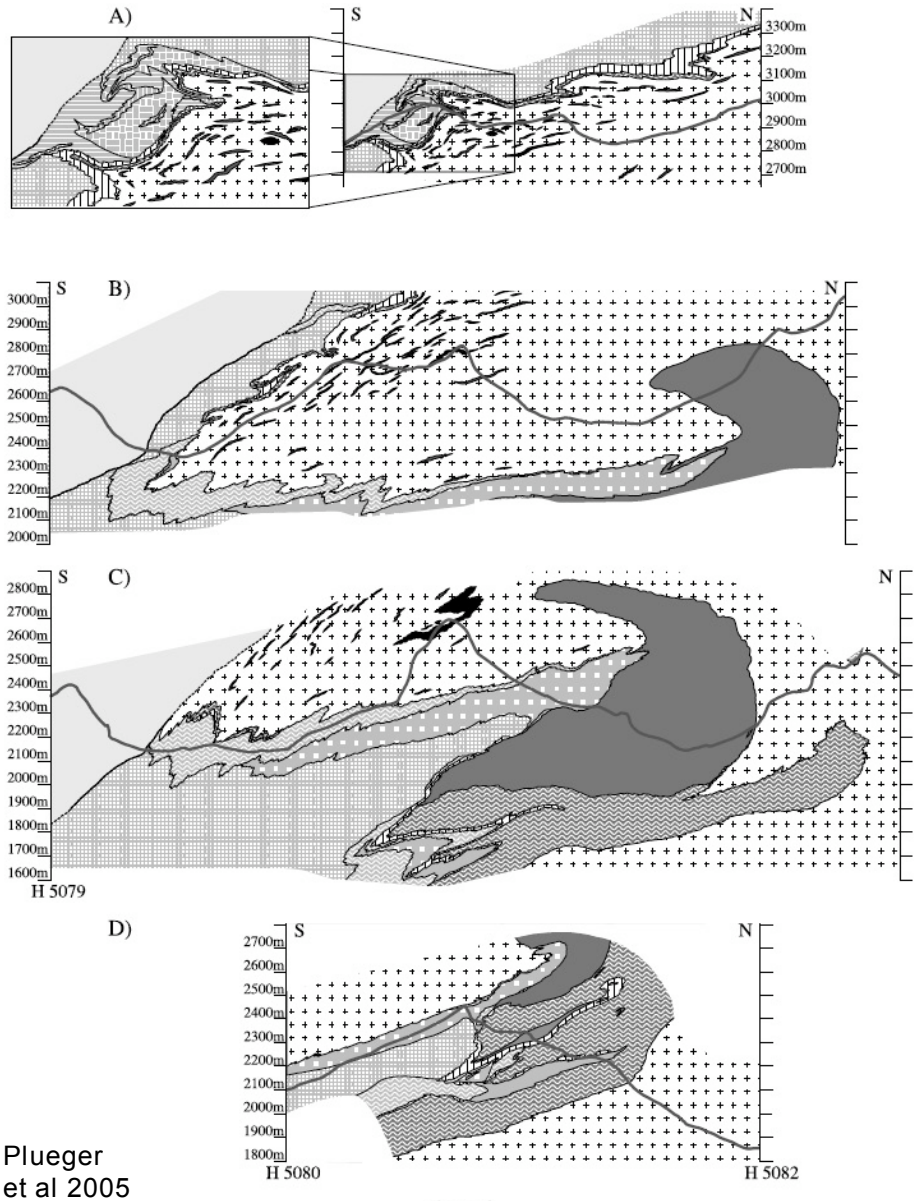

Figure 8

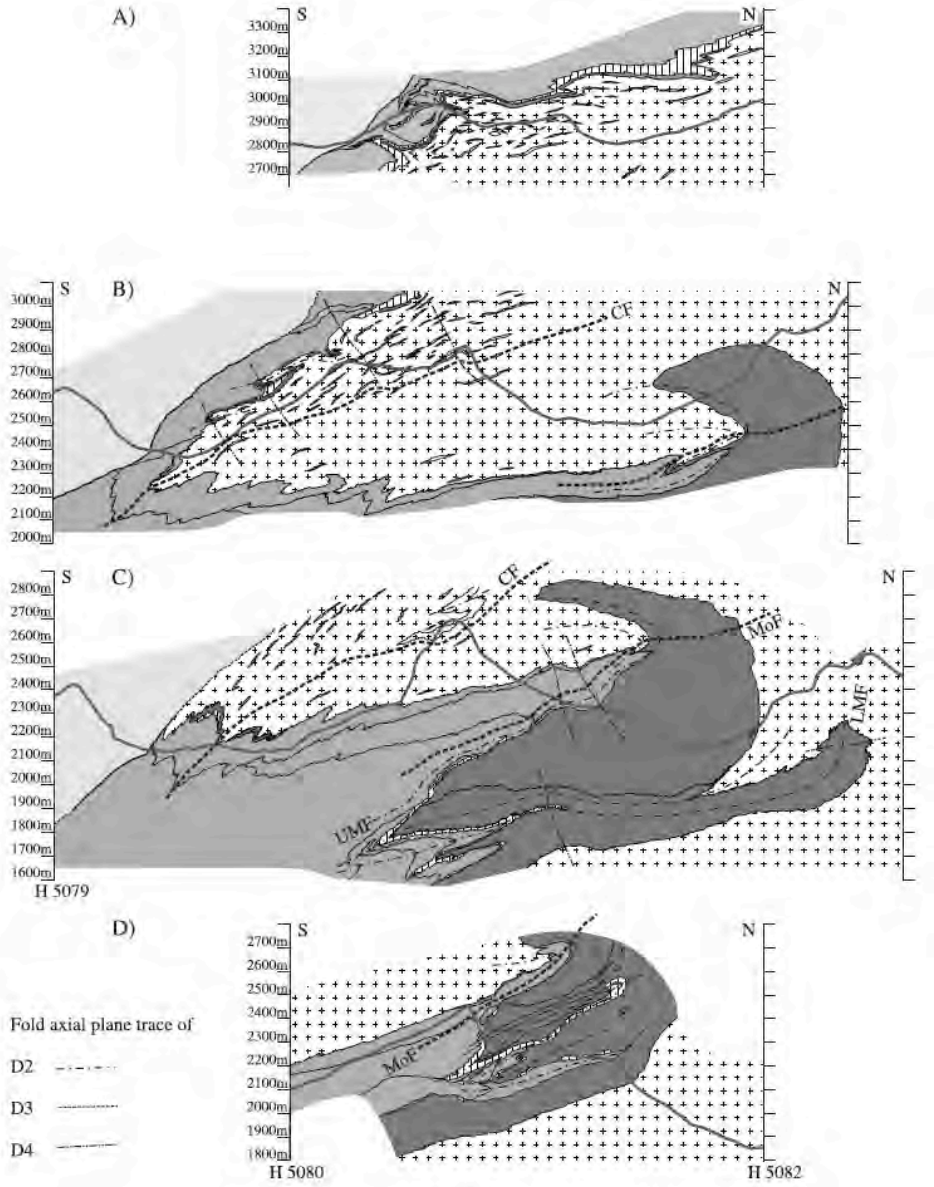

Figure 9

Plueger et al 2005

Figure 8. North-south cross sections (traces, see Figure 7). The patterns are the same as in Figure 6. (a) Cross section through Corno del Camoscio in the normal-lying upper limb of the Cimalegna fold. The enlarged section shows the complex geology of Corno del Camoscio. (b) Cross section through central parts of the Cimalegna comprising the Cimalegna fold and the upper Malfatta fold with Balma eclogites of maximal thickness in its core. (c) Cross section through eastern parts of the Cimalegna. Below the Cimalegna fold, ophiolites of the Zermatt-Saas and Balma unit are separated by an incoherent band of Stolemberg gneisses. (d) Cross section west of Corno d'Olen. Compared to Figure 8c, the ophiolitic units are less thick, especially the eclogites of the Balma unit wedge out toward east.

Figure 9. Tectonic interpretation of the north-south cross sections as shown in Figure 8. The patterns are the same as in Figure 2. (a) Tight south vergent folds which are partly D_2, partly D_3. They are overprinted by D_4 folds; for example, the Corno del Camoscio is positioned in the steep southern limb of a large D_4 anticline. The Balma and Stolemberg units disappear only sporadically. The boundary between the Tsaté nappe and the Zermatt-Saas zone is poorly exposed but cuts the layering of the Zermatt-Saas rocks. (b) Frontal parts of the Cimalegna fold (CF). Rocks of the Balma and Stolemberg units are restricted to the cores of some tight to isoclinal D_2 and/or D_3 folds. (c) Malfatta folds (UMF, LMF) clearly overprinted by D_3 folding (Cimalegna fold). In the upper limb of the Cimalegna fold, the Tsaté nappe was not involved into D_2 and D_3 folding but emplaced upon the Monte Rosa gneisses during D_4 southeast directed detachment. (d) D_2 fold axial planes that dip slightly steeper toward south than parasitic structures of the large D_3 north closing fold.

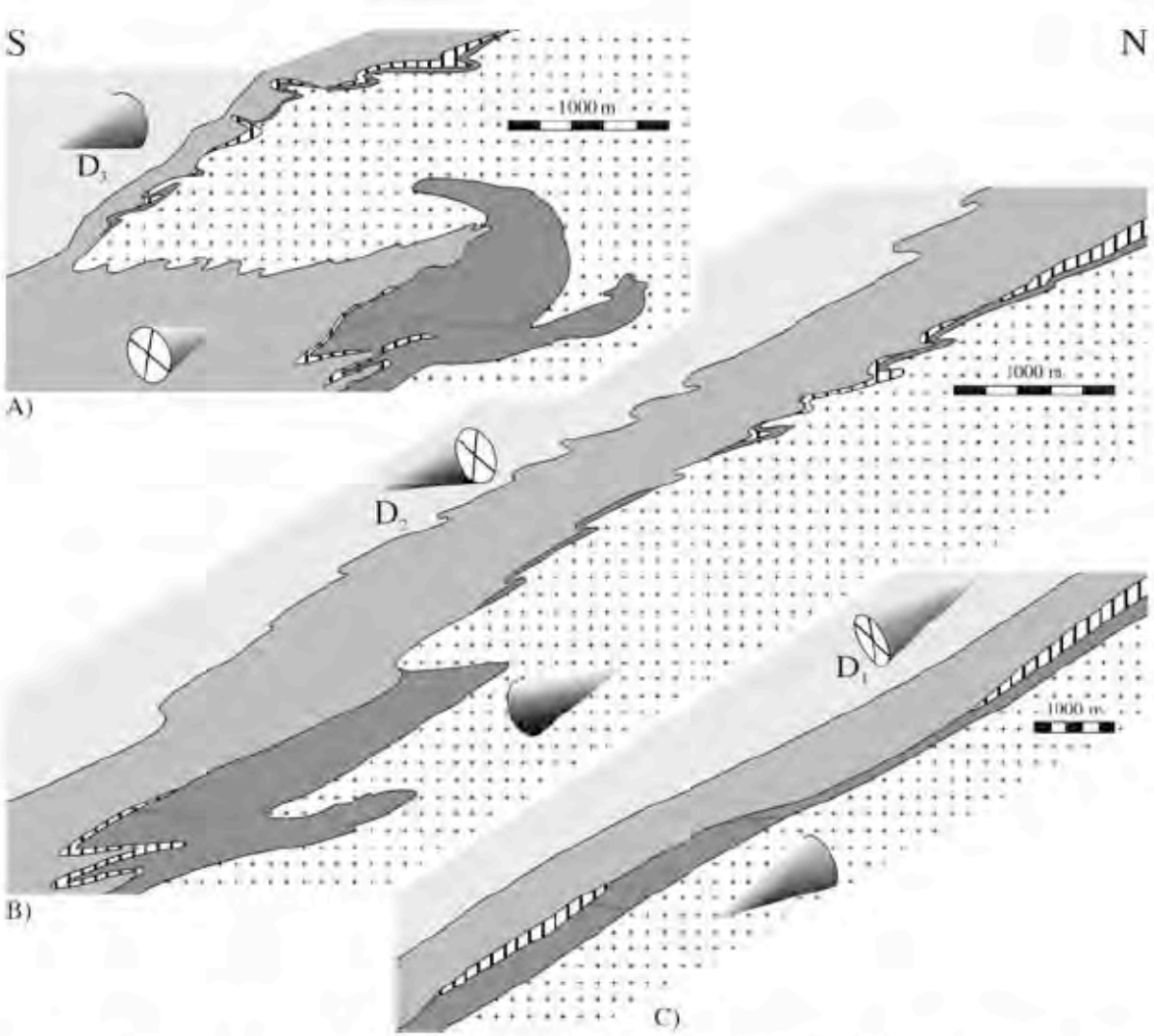

Figure 17. Stepwise retrodeformation of folding and shearing events on the southern side of Monte Rosa. The according part is marked by a dashed rectangle in Figure 18. Patterns are as in Figure 2. Cones indicate directions and senses of shearing which were oblique to the plane of cross section during D_1 to D_3. (a) Present-day situation. (b) Situation after D_2, showing southwest vergent D_2 folds. (c) Situation after D_1, showing the nappe stack comprising Monte Rosa, Balma, Stolemberg, Zermatt-Saas, and Tsaté nappes, from base to top. Note different scale in Figure 17c.

Plueger
et al 2005

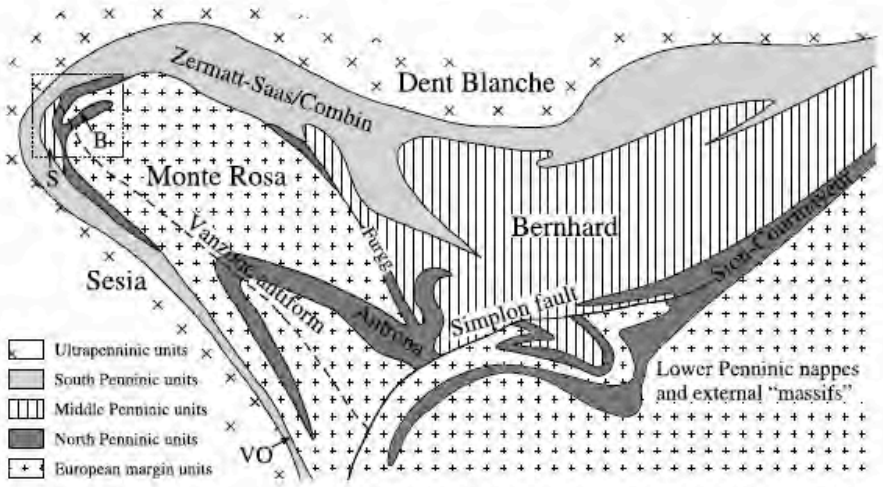

Figure 18. Schematic cross section illustrating a paleogeographic restoration of the Penninic nappes according to results of this study. Dashed rectangle indicates part of the section retrodeformed in Figure 17. VO, suture of the Valais (North Penninic) ocean. Ophiolites at the southern border of the Monte Rosa nappe are interpreted to represent a double suture of the Valais (Balma unit, B) and Piemont-Liguria oceans, with remnants of the Briançonnais (Stolemberg unit, S) in between. Farther north, the Valais suture is represented by an ophiolite layer in the Furgg zone, the Antrona zone, and, offset along the Simplon line, the Sion-Courmayeur zone. The Monte Rosa nappe is the southernmost exposed part of the European continental margin.

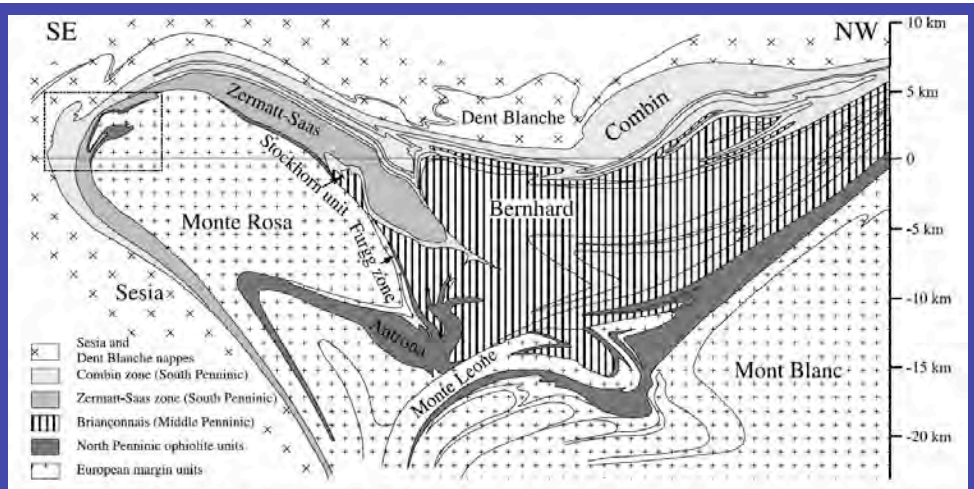

Figure 2. Cross section through the western Swiss-Italian Alps, modified after *Escher et al.* [1993]. The units are combined according to their paleogeographic origins proposed in this paper. Thin black lines within tectonic units are second-order nappe boundaries and lithological boundaries which are shown in order to highlight the internal structures. Dashed rectangle indicates approximate location of the study area.

Plueger
et al 2005

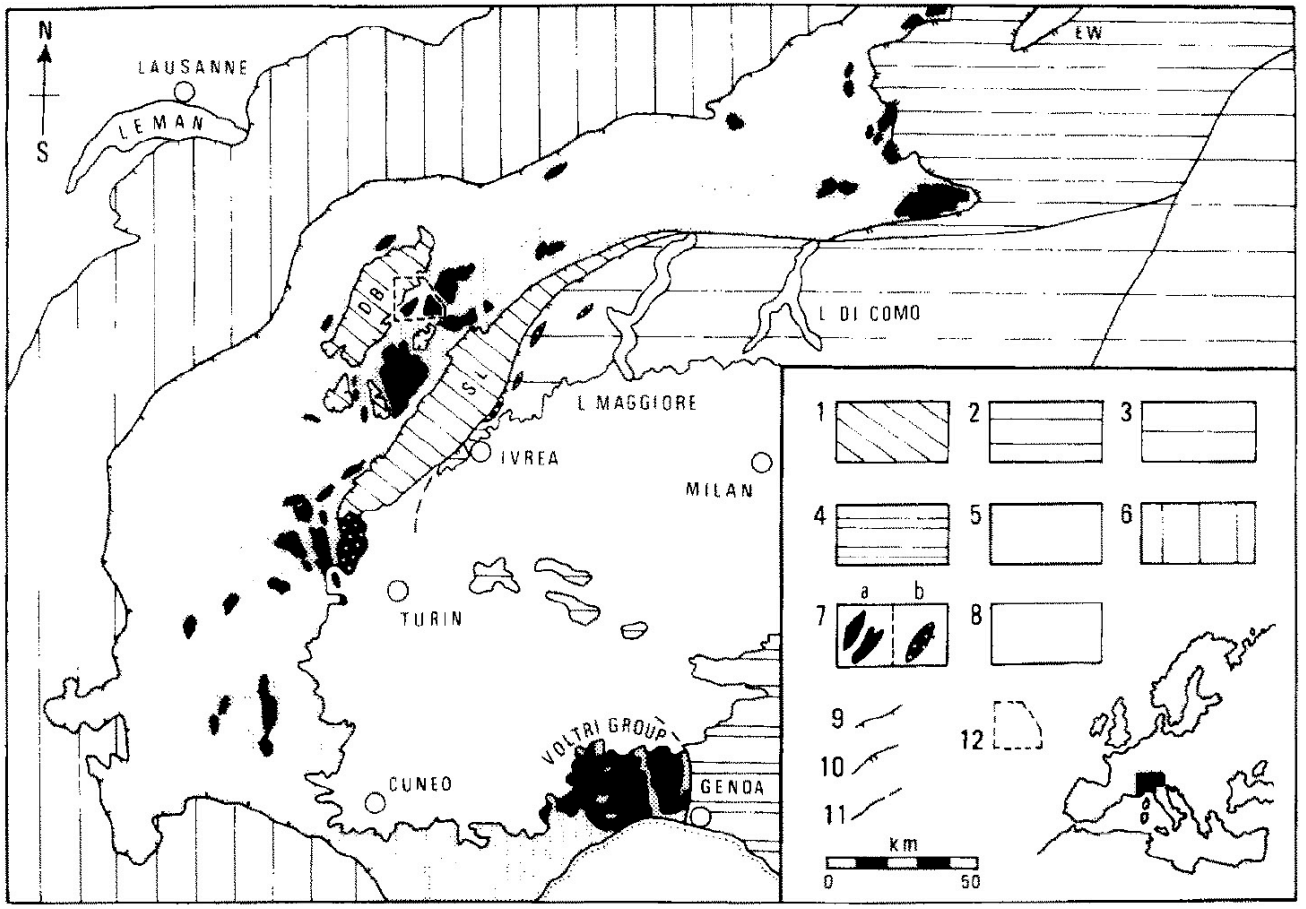

Fig. 1. Tectonic sketch map of the Western and Central Alps. Nappe overturning is directed externally, away from the Po Plain. The paleogeographic and structural realms are represented as follows: (*1*) Austroalpine tectonic system of the Western Alps, including the Sesia—Lanzo (*SL*) and the Dent Blanche (*DB*) composite nappes; (*2*) eastern Austroalpine realm; (*3*) Southern Alpine terrane; (*4*) Northern Apennines; (*5*) Pennine Zone, including the Piemonte ophiolite nappe; (*6*) Helvetic and Ultra-helvetic realm, including nappes of the Prealps. Differentiated lithologies: (*7*) periodotites and serpentinized equivalents (*a*) chiefly from the Piemonte ophiolite nappe, and (*b*) principally from South Alpine Ivrea Zone and including the Lanzo massif. (*8*) Middle Oligocene and younger molasse. (*9*) Main thrust planes, barbs on the upper unit. (*10*) Alpine Suture, and internal boundary of the early Alpine high-pressure, low-temperature metamorphism in the Western Alps. (*11*) Major high-angle faults (Insubric, Giudicarie and Sestri—Voltaggio Lines). *EW*: Engadine window. The dashed line indicates the location of the Breuil—St. Jacques area of Fig. 3.

Dal Piaz and Ernst 1979

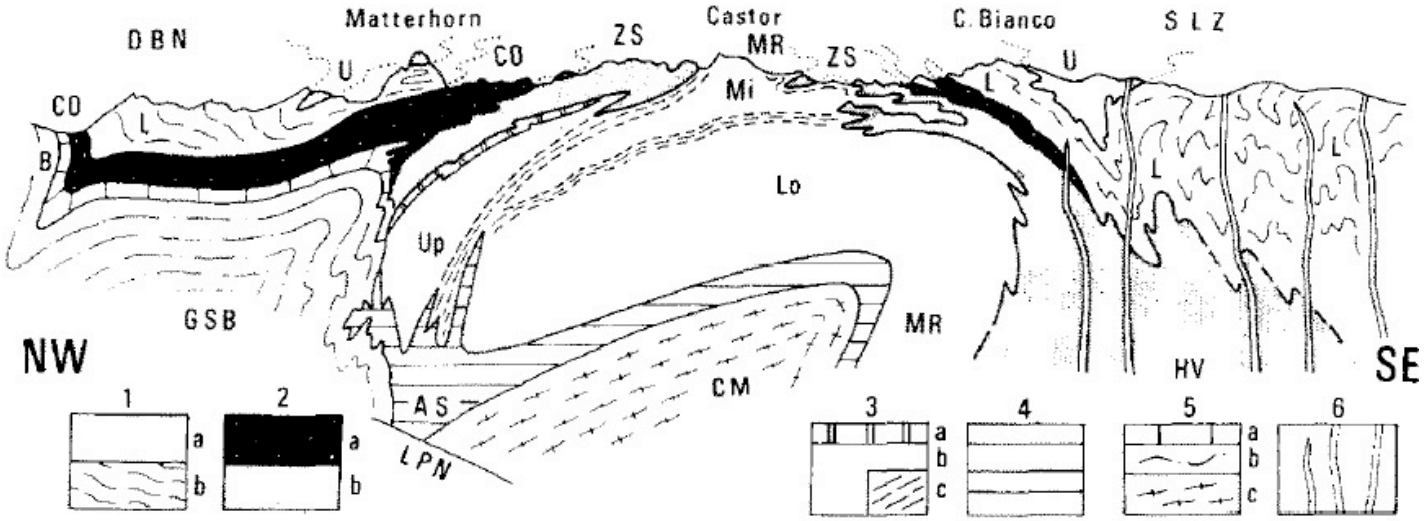

Fig. 2. Cross-section through the internal northwestern Alps between the Valais and the lower Aosta Valley, partly after Bearth and Lombard (1964), Dal Piaz (1965, 1976), Dal Piaz et al. (1972), Milnes (1974a, b), Klein (1975), and Compagnoni et al. (1975). It is a part of profile "C" through the Alps being constructed in collaboration with G. Gosso under the auspices of the I.G.C.P. (*1*) Austroalpine tectonic system, including the Dent Blanche (*DBN*) and the Sesia-Lanzo (*SLZ*) composite nappes: (*a*) the upper tectonic unit (*U*), comprising the Valpelline Series and the II Diorito—Kinzigitica zone; (*b*) the lower tectonic unit (*L*), consisting of the Arolla Series and the eclogitic micaschists + gneiss minuti complexes. (*2*) Piemonte ophiolite nappe (Tethyan suture): (*a*) the overlying Combin unit (*CO*); (*b*) the underlying Zermatt—Saas unit (*ZS*), grading in the lower right-hand portion of the profile to the undifferentiated high-velocity zone (*HV*) of "Berckhemer's beak" (Giese et al., 1970), which corresponds to mainly ultramafic slices derived from the upper mantle and lowemost crust. (*3*) Pennine Monte Rosa nappe (*MR*): (*a*) Permian—Mesozoic sedimentary cover of the Gornergrat zone; (*b*) undifferentiated crystalline basement; (*c*) Furggen zone and shear horizons. Three main tectonic units can be discerned within the Monte Rosa nappe: the upper Portjegrat zone (*Up*), the middle Castor-Lyskamm zone (*Mi*) and the lower undifferentiated unit (*Lo*). (*4*) Antrona ophiolitic syncline (*AS*). (*5*) Pennine Gran San Bernardo nappe (*GSB*): (*a*) the Briançonnais sedimentary cover (*B*), which does not display ophiolitic sequences; (*b*) crystalline basement, including the Permian—Carboniferous section; (*c*) Camughera and Moncucco tectonic units (*CM*). *LPN*: problematic lower Pennine nappes. (*6*) Andesite and lamprophyre dikes of Oligocene age, postdating the continental collision and the Lepontine metamorphism.

Dal Piaz and Ernst 1979

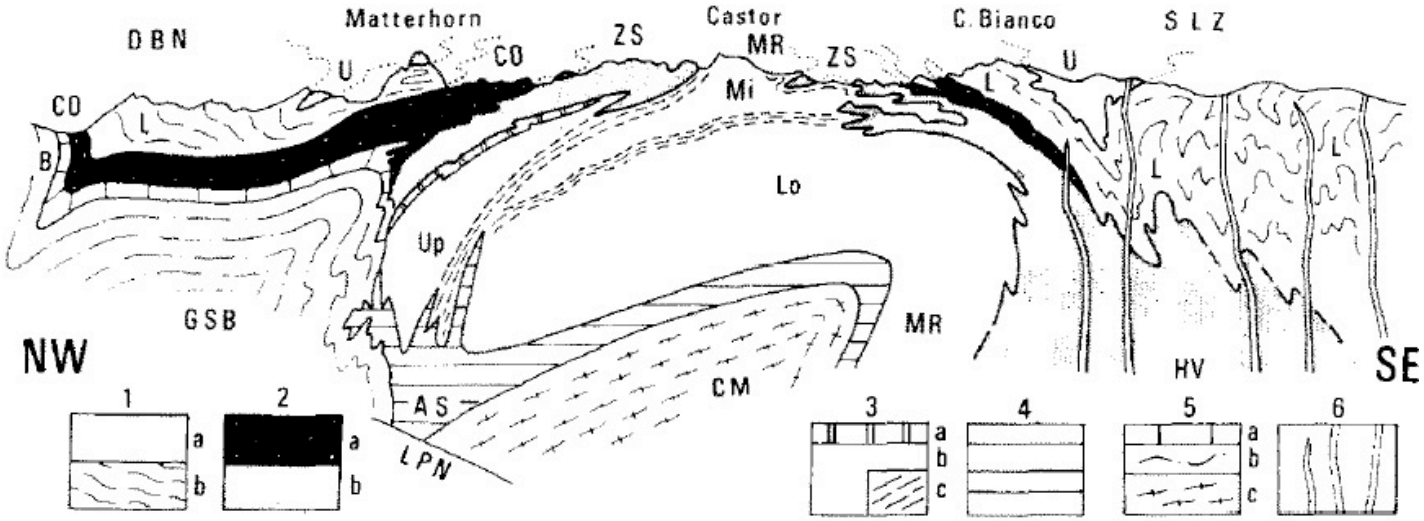

Fig. 2. Cross-section through the internal northwestern Alps between the Valais and the lower Aosta Valley, partly after Bearth and Lombard (1964), Dal Piaz (1965, 1976), Dal Piaz et al. (1972), Milnes (1974a, b), Klein (1975), and Compagnoni et al. (1975). It is a part of profile "C" through the Alps being constructed in collaboration with G. Gosso

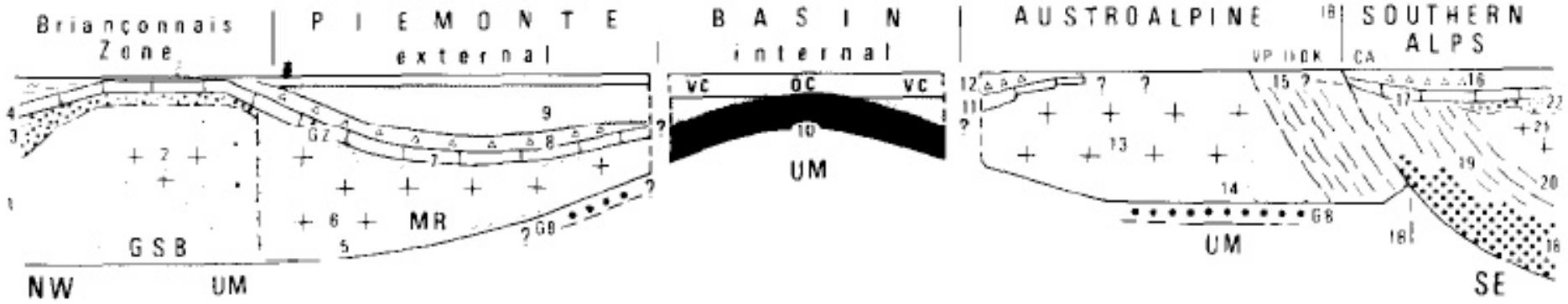

Fig. 4. Palinspastic and lithostratigraphic reconstruction of the Piemonte basin and surrounding realms along the cross-section of Fig. 2, at about the Jurassic—Cretaceous time boundary.

cover (*B*), which does not display ophiolitic sequences; (*b*) crystalline basement, including the Permian—Carboniferous section; (*c*) Camughera and Moncucco tectonic units (*CM*). *LPN*: problematic lower Pennine nappes. (*6*) Andesite and lamprophyre dikes of Oligocene age, postdating the continental collision and the Lepontine metamorphism.

Dal Piaz and Ernst 1979

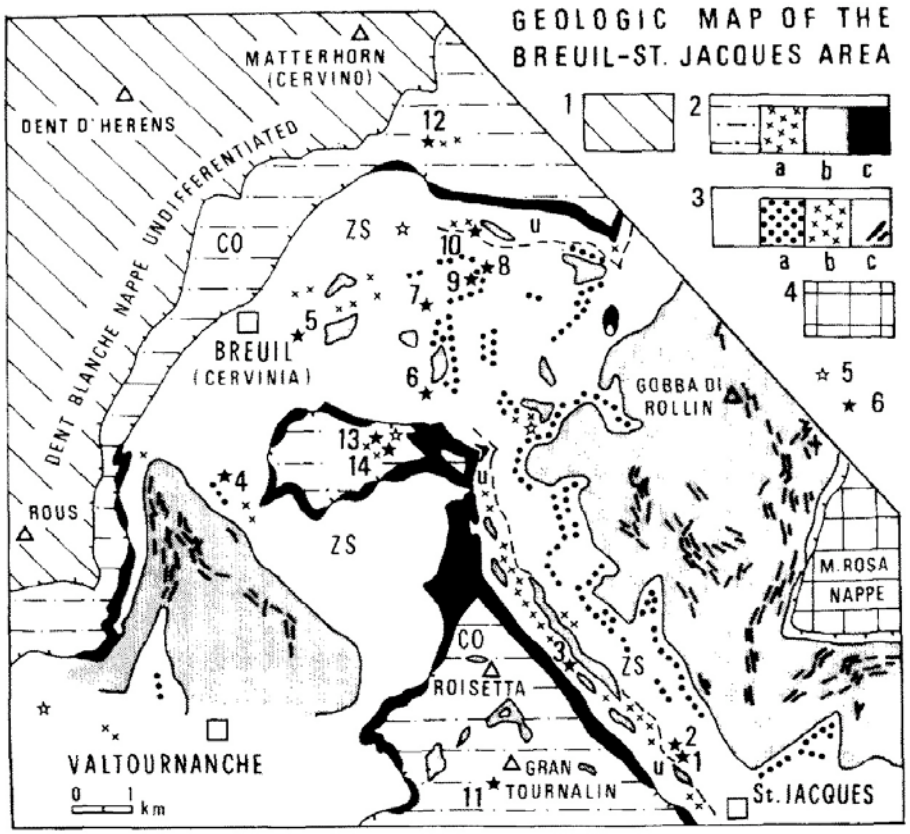

Fig. 3. Tectonic and lithologic scheme of the Breuil—St. Jacques area, the regional setting of which is shown in Fig. 1. (*1*) The Austroalpine Dent Blanche nappe, undifferentiated. (*2*) The Combin unit (*CO*) of the Piemonte ophiolite nappe, mainly consisting of calc-schists and interbedded prasinites: (*a*) metagabbro lenses; (*b*) serpentinite lenses; (*c*) pre-ophiolitic sedimentary basal complex, including Permian (?) metaconglomerates and schists, Triassic quartzites and carbonates, Liassic sedimentary breccias and calc-schists. The Combin unit shows a greenschist facies metamorphic overprinting. (*3*) The Zermatt—Saas unit (*ZS*) of the Piemonte ophiolite nappe: undifferentiated basaltic metabasites, ankeritic mica schists with rare marbles and metacherts; (*a*) Garten—Rifelberg Formation; (*b*) metagabbros; (*c*) pervasively serpentinized ultramafites and rodingitic dikes (black). An upper tectonic sheet (*u*) has been distinguished locally within the Zermatt—Saas unit (Dal Piaz, 1965). The Zermatt—Saas unit displays an early eclogitic stage of metamorphism, succeeded by glaucophanic, barroisitic and actinolitic phases of retrogression. (*4*) Pennine Monte Rosa nappe, undifferentiated. (*5*) Manganiferous piemontite + garnet-bearing metacherts in both Zermatt—Saas and Combin units; blocks of the northern Mn-rich layer occur within a big landslide derived from the Teodulo—Furggen crest (Combin unit). (*6*) Location of analyzed samples: *1* = specimens MRO-1105 and MRO-1109; *2* = MRO-857; *3* = MRO-1756; *4* = DBL-409; *5* = MRO-1609, MRO-1611 and MRO-1624; *6* = DBL-379; *7* = MRO-1634; *8* = DBL-497; *9* = DBL-488; *10* = DBL-547; *11* = MRO-1783; *12* = DBL-628; *13* = DBL-515; *14* = DBL-510.

Dal Piaz and Ernst 1979

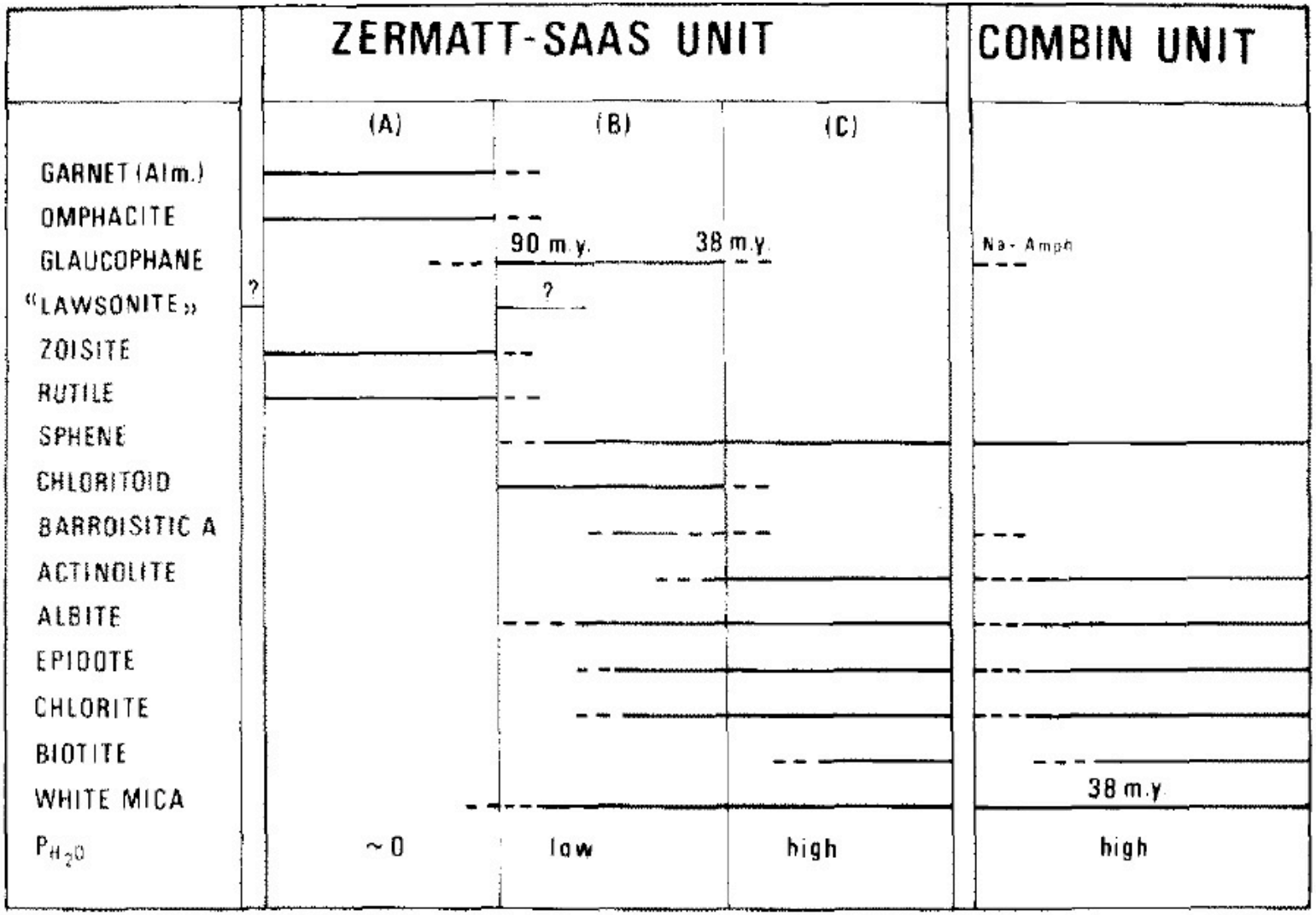

Fig. 5. Schematic diagram showing mineral assemblages and metamorphic stages in the Zermatt—Saas and Combin units from the Breuil—St. Jacques area. Dashed lines signify rare or questionable occurrences. The persistence of metastable relics is not represented. Stage *A* is early, *B* intermediate and *C* late in the recrystallization continuum. Combin rocks contain mineral assemblages characteristic of stage *C* only.

Dal Piaz and Ernst 1979

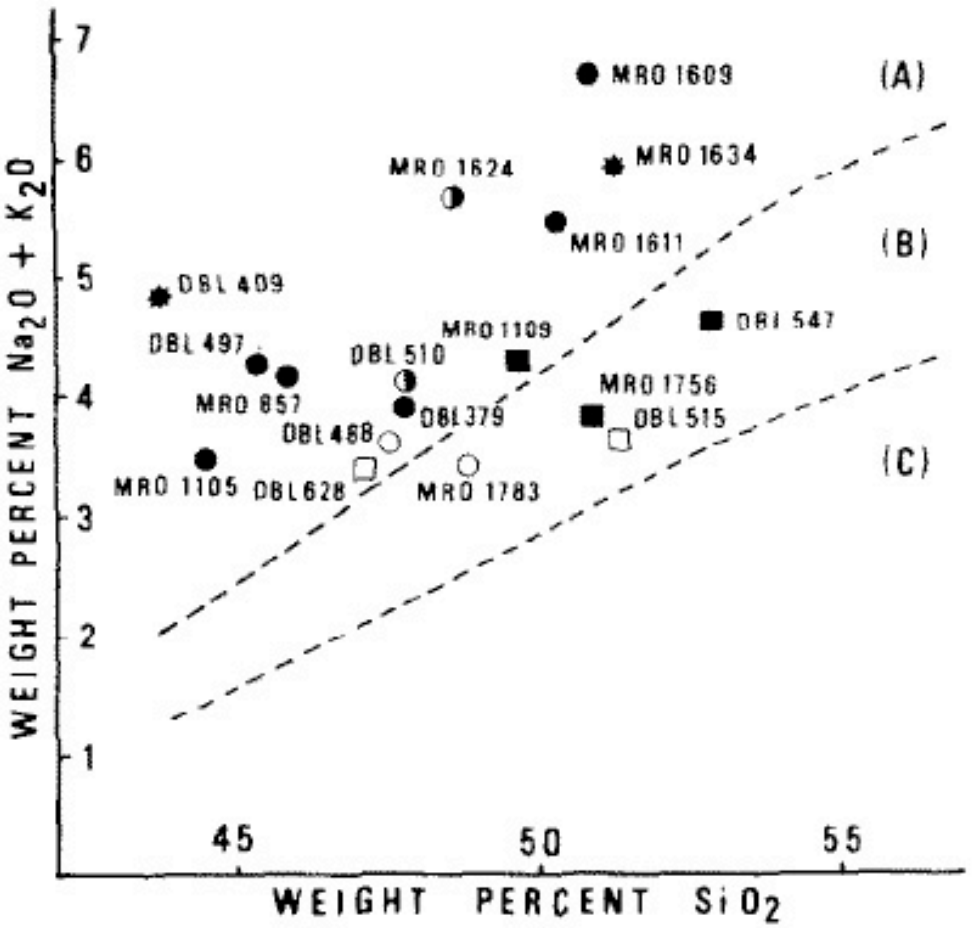

Fig. 7. Plot of total alkalis versus silica for bulk rock analyses presented in Tables I and II. Symbols represent lithologic types as follows: (1) Zermatt—Saas unit: eclogites and glaucophane-eclogites (= large, solid circles); garnet-glaucophanites (= solid asterisks); thoroughly retrograded eclogites (= half-solid circles); metagabbros (= solid squares). (2) Combin unit: prasinites (= open circles) and metagabbros (= open squares). Fields *A*, *B* and *C* represent compositional variations for fresh alkali, high-alumina and tholeiitic basalts, respectively (Kuno, 1960, 1966).

Dal Piaz and Ernst 1979

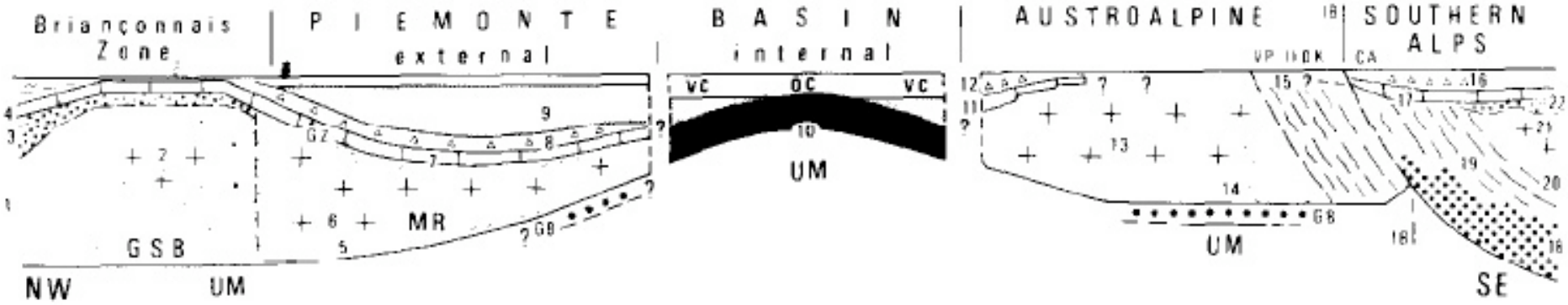

Fig. 4. Palinspastic and lithostratigraphic reconstruction of the Piemonte basin and surrounding realms along the cross-section of Fig. 2, at about the Jurassic—Cretaceous time boundary.

Dal Piaz and Ernst 1979